STATISTICAL PROPERTIES OF SEQUENTIAL DETONATION SYSTEMS

by

THEODOR DANIëL WINTER

DISSERTATION

submitted in the fulfilment
of the requirements for the degree

MASTER OF SCIENCE

in

STATISTICS

in the

FACULTY OF SCIENCE

at the

RAND AFRIKAANS UNIVERSITY

SUPERVISOR : PROF F LOMBARD

NOVEMBER 1996

Sequential detonation systems play an important role in mining. Manufacturers and consumers of detonators that are used in these blasting sequences are concerned with certain statistical properties of such sequential configurations. Two properties of particular interest are the *probability of reversal* and the *initiation front*. Statistical models describing these properties can be developed if the delay times of the detonators are normally distributed. This enables one to construct various quality control procedures to monitor these properties.

Sekwensiële ontploffingstelsels speel 'n belangrike rol in die mynbedryf. Sekere statistiese kenmerke van 'n sekwensiële ontploffingsproses is van belang vir beide vervaardigers en verbruikers van die ontstekingstoestelle wat in die proses gebruik word. Twee kenmerke is van spesifieke belang: die *mislukkingswaarskynlikheid* en die *ontstekingsfront*. Indien die brandtye van die ontstekers normaal verdeel is, kan daar statistiese modelle ontwikkel word wat die bogenoemde kenmerke beskryf. Sodoende kan daar kwaliteitbeheer prosedures opgestel word wat hierdie kenmerke beheer.

This dissertation would have stopped on this page, were it not for the constant encouragement, motivation and support of professor F. Lombard. The words, equations, theorems and graphs on the pages to follow are but an imperfect attempt to capture on paper some of the insights I have come to during our countless discussions and cups of tea.

If you see a formula in the Physical Review that extends over a quarter of a page, forget it. It's wrong. Nature isn't that complicated. Bernd T. Matthias.

*The words **figure** and **fictitious** both derive from the same Latin root, **fingere — beware!*** M.J. Moroney

Table of contents

1. Introduction and Objectives

1.1. Objectives

At the very roots of this dissertation lies a commercial process with many as yet unexplored characteristics that will be thoroughly examined, using a rich variety of statistical methods and techniques. Broadly speaking, the main objective of this study involves the development of techniques to control the quality of advanced explosives detonators used in commercial mining operations. To accomplish this task, various statistical characteristics of this detonation process are described and examined in order to obtain a holistic understanding of the underlying process. The parameters of the process are introduced and estimates for unknowns are derived. Real-time quality control techniques based on these results are suggested.

1.2. The role of blasting in mining

A major part of South Africa's economy is based on the mining of the rich mineral deposits that are to be found in the country. These mining operations are carried out both above ground (open-pit iron ore mines, for example) and below ground (gold, uranium and others).

Open-pit mining, in particular, requires significant amounts of commercial blasting to dislodge the high volumes of material that have to be moved and processed. An average blasting block at Iscor's Sishen mine, for example, contains

about 250 000 tons of material, although a world record was established in April 1981 when 7,2 million tons of rock was broken during a *single* blast.

The chemical quality of the final products is partly controlled by supplying the primary crusher at the mine with a suitable mixture of so-called run-of-mine ore. To determine which material from a specific blasting block may be sent to the plant, and to which waste dump the remaining material should be assigned, factors such as beneficiation properties of the raw material and the content of various by-products are considered.

Samples are typically taken from alternate blast holes for every metre drilled. Each drill sample is divided into two parts by means of a riffler for a washed and unwashed sample. The washed samples are examined and the rock types noted. Subsequently, all the samples are grouped and analysed chemically and the densities of the different rock types are determined. The results are processed and those for the washed and unwashed samples correlated.

The blasting blocks in the pit are demarcated by means of whitewash lines, according to the divisions on the blasting-block plans, and they are marked with signs to guide shovel operators. Primary drilling is performed by means of electrically-driven rotary drills. At the Sishen mine, 310 mm diameter blast holes are drilled in all rock types. The following table depicts typical drilling

patterns for various rock types:

Rock type	*Pattern (m)*	*Drill depth (m)*
Hard iron ore	$7,2 \times 8,3$	$3,0$
Medium-hard iron ore	$8,1 \times 9,3$	$2,7$
Quartzite	$8,2 \times 9,4$	$2,5$
Flagstone	$8,2 \times 9,4$	$2,5$
Calcrete	$8,1 \times 9,3$	$3,0$

(1.1)

Primary blasting is done at Sishen with *Heavy Anfo*, an explosive that is manufactured by mine personnel at the emulsion plant on site. The ingredients for the explosive blends are transported by pump trucks to the blasting blocks, where it is mixed and pumped down the blast holes.

Good fragmentation of the blasted material is a prerequisite for high loading rates by the loading equipment. At Sishen and other similar mines, a blasting efficiency of $3,2$ tons of rock per kilogram of explosives used, is considered to be acceptable.

1.3. Setting up a blasting sequence

To set up a sequential blasting process, the following steps are followed:

1. A number of holes are drilled into the stopeface, using a particular configu-

ration, and explosive charges are lodged inside the holes. Figure 1.1 illustrates a simple blasting configuration used in a variety of mining operations, such as those found in gold mines. The numerals indicate the sequence in which the charges are to fire.

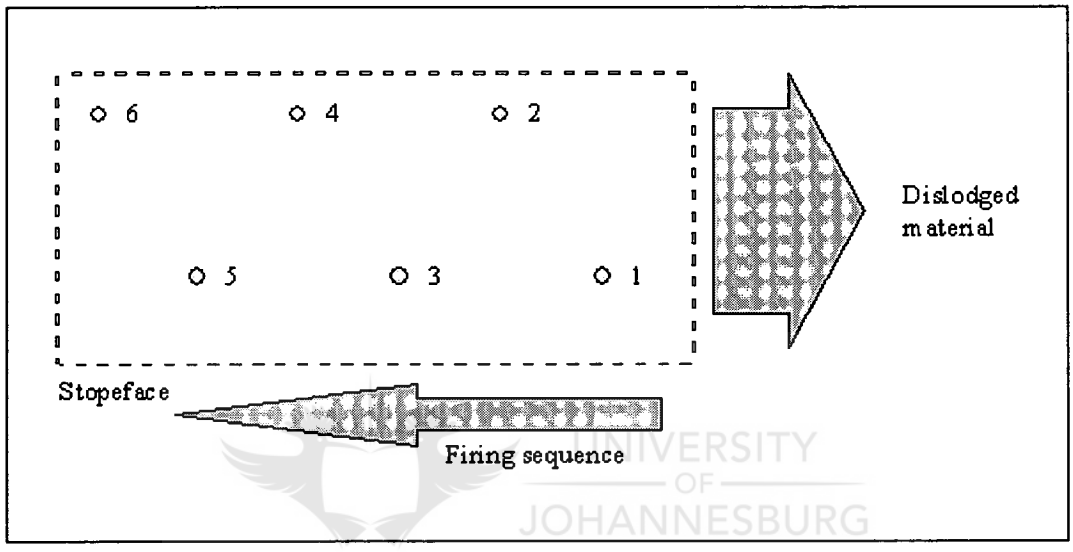

Figure 1.1: Conventional gold mining pattern.

Another typical pattern, commonly used in platinum mines, is depicted in Figure 1.2.

2. Detonators are inserted into the charges. Each detonator consists of a *main delay element*, which causes a delay before setting off a *pyrotechnic* that serves to set off the main explosive charge in the hole. Figure 1.3 schematically depicts the composition of a detonator lodged inside an explosive charge.

3. Connector cords (or "trunk lines") are used to connect the series of det-

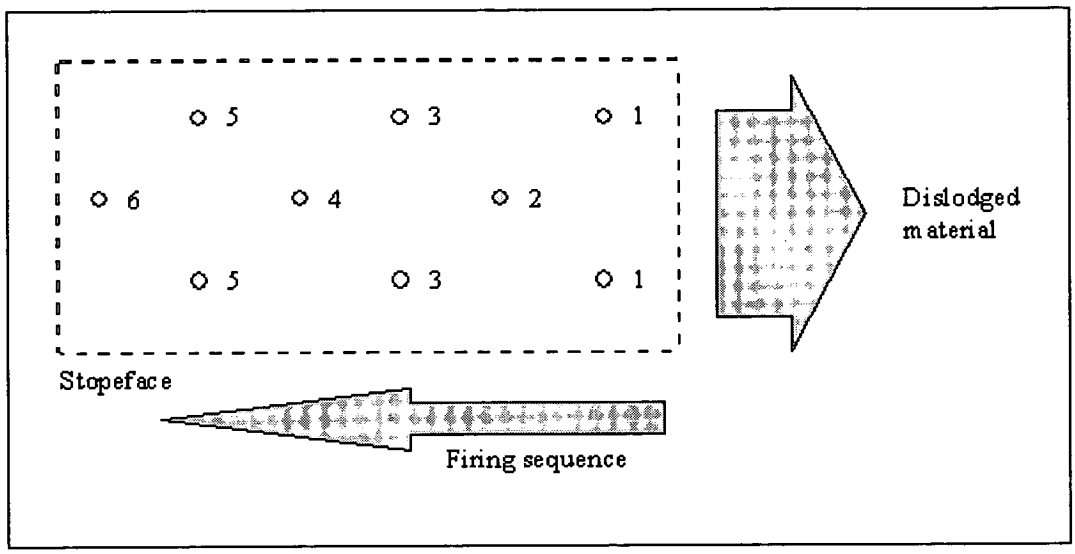

Figure 1.2: Platinum mining blasting pattern

onators. These cords carry the leading "spark" down the array of detonators, igniting them in sequence. Modern connector cords are manufactured in a high technology environment and are extremely reliable and fast. "Shock Tube", for example, is a thin plastic tube, coated inside with a delicate layer of pyrotechnic dust that burns at an incredible rate of 2 000 m/s. The purpose of the main delay element in a detonator is to delay igniting the main charge until the leading spark has moved sufficiently far along, thereby avoiding a possible interruption of the ignition process, such as flying rocks cutting off nearby connector cord that still has to carry the spark.

4. Slight time delays are required between successive explosions to ensure success, since the material around each hole has to explode into the opening

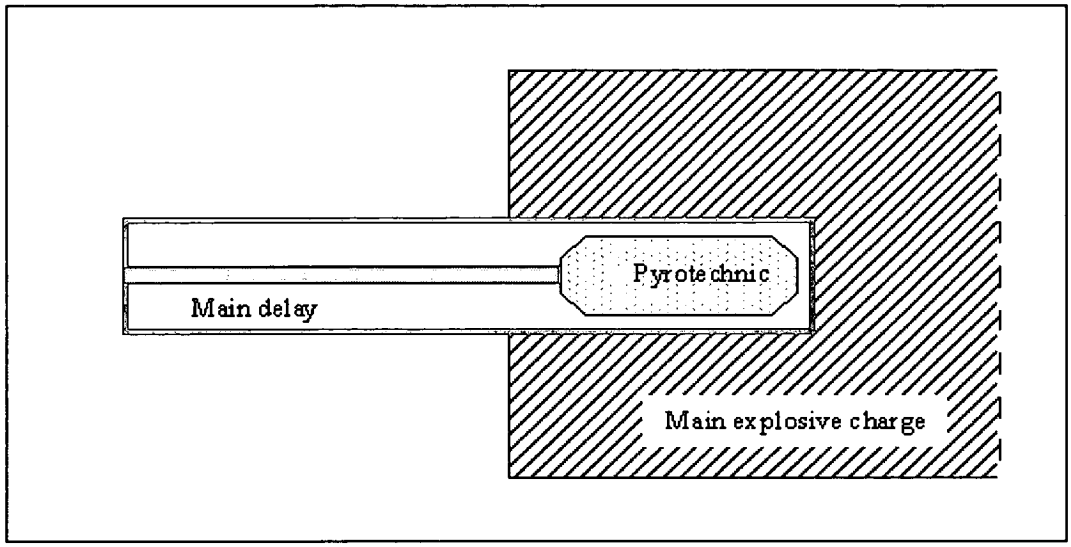

Figure 1.3: Schematic representation of a detonator.

created by the charge in the hole preceding it. To generate these time delays, "surface delays" are placed in between main delays. Figure 1.4 illustrates a typical sequential array of such detonators and explosive charges.

Upon blast initiation, usually via electrical means, the first detonator main delay will be initiated and, simultaneously, the surface delay to the second detonator. This surface delay is much shorter than the first main delay, so that it will initiate the second main delay shortly after initiation of the first one. This process is repeated, with successive surface delays causing delays between the ignition of main delays. When the first detonator eventually explodes, the others will follow quickly. By this time the surface delay currently burning will be some way ahead of the exploding charges, with all the main delays in between having

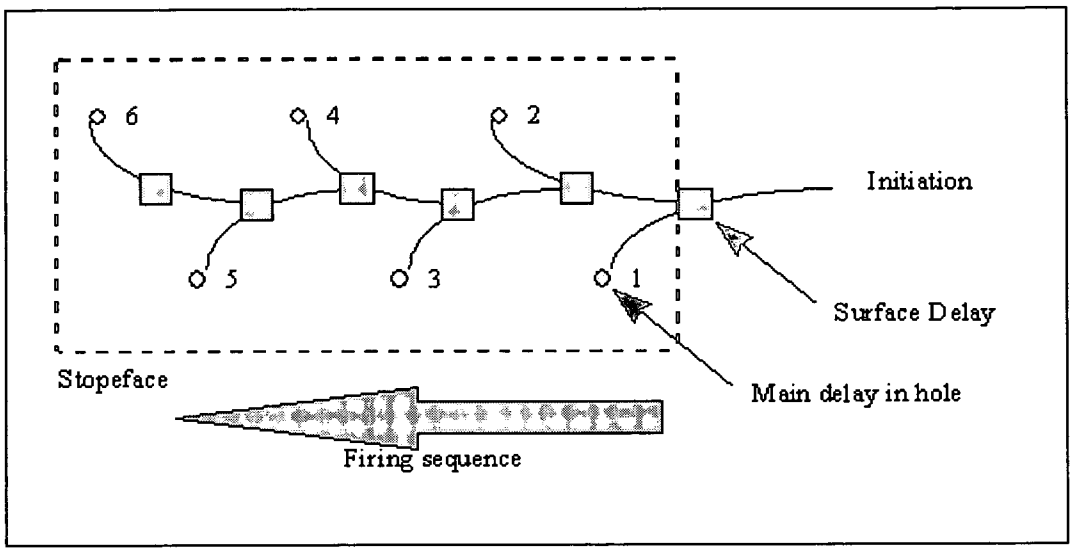

Figure 1.4: Sequential array of detonators.

been consecutively ignited.

1.4. Process Properties

Two properties of this sequential array of explosions are of extreme importance, namely the *probability of reversal* and the *initiation front.*

1.4.1. The Probability of Reversal

Many different blasting patterns exist for the various types of mining operations and geological characteristics of a particular mining area. All these blasting patterns, however, prescribe a particular sequence of detonation. If a certain charge or charges explode out of sequence, for whatever reason, the whole blast could be

compromised, or its ultimate effect vastly reduced, leading to substantial economic losses. Both the manufacturer and end-user of detonators are therefore concerned with the probability of such out-of-sequence explosions, or *reversals*, taking place. A major objective of this study will be to develop and state important quality control results in terms of the probability of reversal within the frame of reference of the manufacturer and consumer.

1.4.2. The Initiation Front

As was stated earlier, the surface delays are chosen to be of much shorter length than the main delays. The reason for this is to ensure that the ignition process is always a number of main delays ahead of the explosion process. The number of ignited main delays ahead of the charge that is to explode next is referred to as the *initiation front* (or *burning front*).

As will be seen later, there is a direct trade-off between the length of the initiation front and the probability of reversal, with longer (safer) initiation fronts implying higher reversal probabilities and vice versa.

1.5. Delay Time Distributions

The burning time of a delay depends on the physical properties of its composite materials, such as the density and homogeneity of its chemical fuse, cut length, temperature, etc. Since it is usually not possible to manufacture detonators that

have the exact same physical properties in all respects, one would expect their various burning times to be subject to statistical variation. It is this variation that results in a non-zero probability of reversal arising under certain circumstances. Continuing advances in mining technology, such as the development of economically viable electronic detonators, will keep improving the quality obtainable in a detonation process (reduced probability of reversal coupled with longer initiation front).

To develop statistical quality control techniques that will monitor detonator quality, some initial assumptions about the distribution of delay times have to be made. Traditionally, these have been assumed to be normally distributed. In most practical quality control situations slight deviation from normality does not have a material effect on quality, because of the law of large numbers and the central limit theorem. In this case, however, as will be shown later, even slight deviation from normality in the tail areas result in notable increases in reversal probabilities. Some attention will therefore be paid to the development of real-time procedures to test for deviation from normality.

1.6. Literature Survey

In 1967 Trollip et al calculated a probability of reversal for a pair of detonators. Apart from this, no further work on the subject has been published in the general

scientific literature. However, an extensive literature search did produce references to internal documents of a number of South African and foreign companies involved in mining or explosives production. Due to the confidential nature of these documents, they were unavailable for review.

Ensign-Bickford Co., the largest manufacturer of explosives in the USA, was also consulted on further literature freely available within the industry. They were unaware of any other studies related to the results that are to be stated in this dissertation.

2. The Probability of Reversal

2.1. Introduction

In Chapter 1 it was stated that manufacturers and consumers evaluate the quality of a batch of detonators according to the probability of experiencing a reversal when using such detonators in sequential blasting procedures. In this section I shall formalise the concepts of *reversal* and *pairwise reversal*, as well as propose a mathematical model describing the physical process. Using this framework, point estimators and confidence intervals for the probabilities of these events will be suggested. The bias in the various estimators will also be investigated using Monte Carlo simulation studies, and a method for reducing the bias will be suggested.

2.2. The Conventional Pattern

Figure 2.1 illustrates a conventional sequential blasting pattern of n surface delays and $(n+1)$ main delays, as previously introduced in Figure 1.4.

This arrangement can be schematically represented as in Figure 2.2.

Shaded areas represent time delays. The main delays are labeled $D_1, D_2, \ldots, D_{n+1}$, while the surface delays are labeled $d_1, d_2, \ldots, d_n$.

To illustrate the sequential blasting process, consider the following setup:

- 51 main delays, each burning exactly $3,8$ seconds;

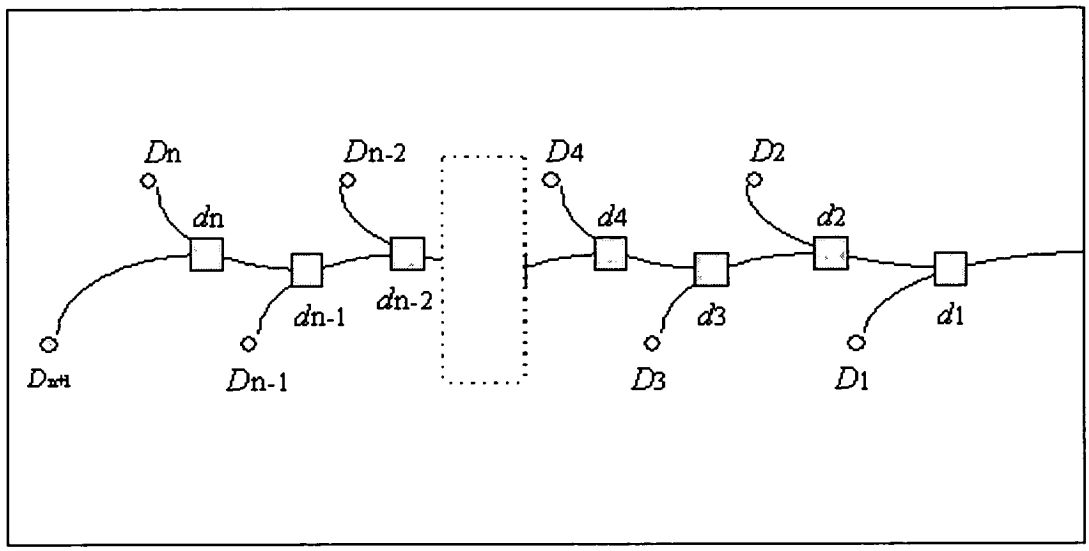

Figure 2.1: Numbered sequential blasting pattern.

- 50 surface delays, each burning exactly $0,2$ seconds.

The following time line describes the process:

Time t	$0,0$	$0,2$	...	$3,8$	$4,0$	$4,2$	...	$9,6$	$9,8$	$10,0$	$10,2$	...	$13,8$	$14,0$
Initiate	d_1	d_2	...	d_{20}	d_{21}	d_{22}	...	d_{49}	d_{50}					
Initiate	D_1	D_2	...	D_{20}	D_{21}	D_{22}	...	D_{49}	D_{50}	D_{51}				
Explode					D_1	D_2	...	D_{29}	D_{30}	D_{31}	D_{32}	...	D_{50}	D_{51}

(2.1)

If the main and surface delays' burning times were not subject to statistical variation, a reversal would, of course, never occur. However, since burning times do vary, the probability of a detonator exploding prematurely will be positive.

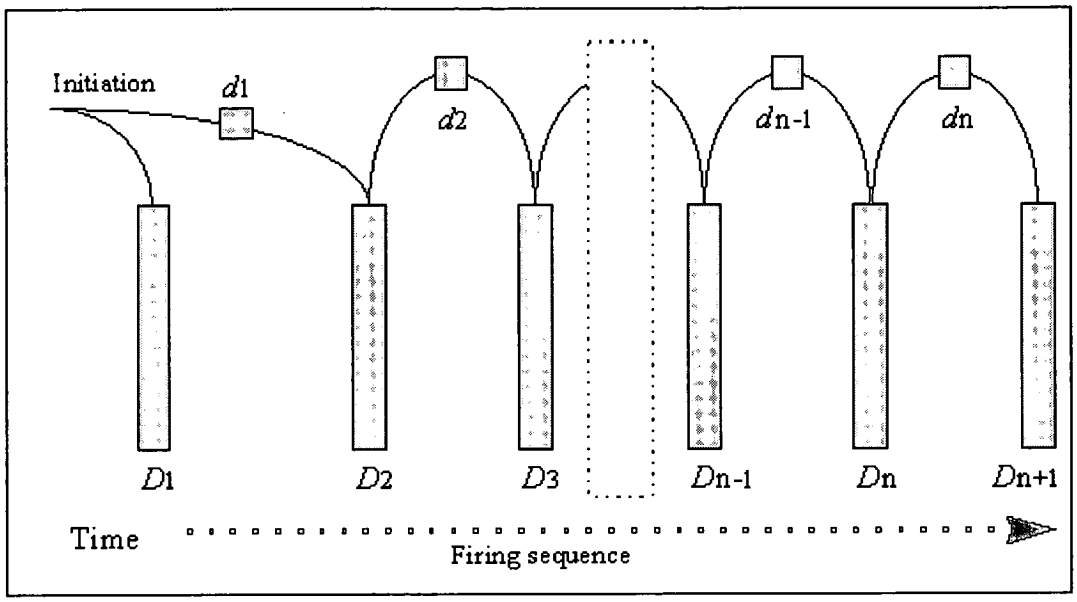

Figure 2.2: Schematic representation of delays.

For the purposes of the results derived in this chapter, I shall assume that the burning times of the main and surface delays are respectively independently identically normally distributed.

Define the random variables

$$\begin{aligned} D_i &=_{\mathcal{L}} N(\mu_D, \sigma_D^2) \quad : \quad \text{Burning time of the } i\text{th main delay} \\ d_i &=_{\mathcal{L}} N(\mu_d, \sigma_d^2) \quad : \quad \text{Burning time of the } i\text{th surface delay} \end{aligned} \tag{2.2}$$

where $=_{\mathcal{L}}$ denotes that the random variable on the left hand side has the distribution indicated on the right hand side, and $N(\mu, \sigma^2)$ denotes the Normal distribution with mean μ and variance σ^2.

Also, define an event

$$R_i := \{A \textit{ reversal occurs at the } i\text{th } \textit{detonator pair}\}. \tag{2.3}$$

Denote the probability of this event by $P(R_i)$. By definition, this shall mean that the $(i+1)$th main delay detonates before the ith main delay. This would happen if, and only if, the aggregate burning time of the ith surface delay and the $(i+1)$th main delay is less than the burning time of the ith main delay.

Now,

$$\begin{aligned}
P(R_i) &= P(d_i + D_{i+1} < D_i) \\
&= P(d_i + D_{i+1} - D_i < 0) \\
&= P\left(\frac{d_i + D_{i+1} - D_i - (\mu_d + \mu_D - \mu_D)}{\sqrt{\sigma_D^2 + \sigma_D^2 + \sigma_d^2}} < \frac{-(\mu_d + \mu_D - \mu_D)}{\sqrt{\sigma_D^2 + \sigma_D^2 + \sigma_d^2}}\right) \\
&= P\left(Z < \frac{-\mu_d}{\sqrt{\sigma_d^2 + 2\sigma_D^2}}\right) \\
&= \Phi\left(\frac{-\mu_d}{\sqrt{\sigma_d^2 + 2\sigma_D^2}}\right) \\
&= \Phi(\lambda) \\
&:= P_{rev}
\end{aligned} \tag{2.4}$$

where

$$\lambda = \frac{-\mu_d}{\sqrt{\sigma_d^2 + 2\sigma_D^2}}. \tag{2.5}$$

P_{rev} is known as the **pairwise** reversal probability and since the formula is

not a function of i, it holds for any consecutive pair of detonators in the sequence.

From (2.4) it is clear that P_{rev} is **not** a function of μ_D, the mean of the main delay times.

Note that λ can be written as

$$\frac{-\mu_d}{\sigma_D}\left(\frac{\sigma_d^2}{\sigma_D^2}+2\right)^{-\frac{1}{2}}. \tag{2.6}$$

Since σ_d^2 is usually much smaller than σ_D^2 in practice, P_{rev} is mainly determined by μ_d, the mean of the surface delays, and σ_D^2, the variance of the main delays. If σ_d/σ_D is assumed to be small enough to be negligible, then (2.4) reduces to

$$P_{rev} = \Phi\left(\frac{-\mu_d}{\sqrt{2}\sigma_D}\right). \tag{2.7}$$

Most quality control procedures are designed to monitor the means μ_D and μ_d, which is not too difficult to accomplish. However, if a manufacturer wants to control the probability of reversal for his product, μ_D is irrelevant — he should be controlling σ_D^2.

Note that σ_D^2 can be reduced by reducing μ_D, but, as will be explained in Chapter 3, this reduces the initiation front, which has other negative operational implications.

Figure 2.3 depicts P_{rev} for $\mu_d = 200$ ms.

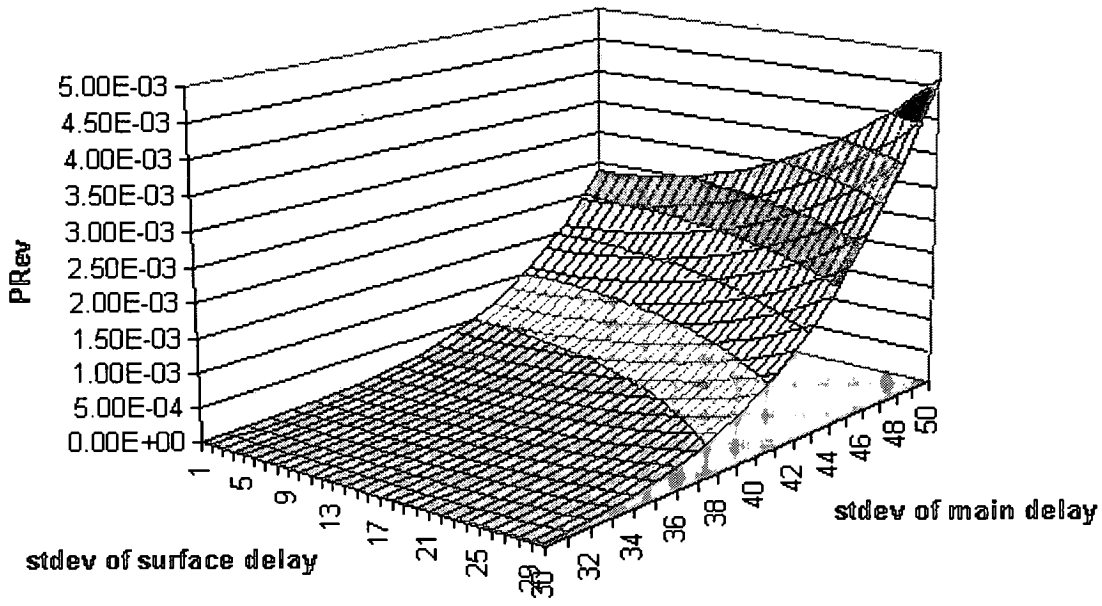

Figure 2.3: Pairwise probability of reversal, $\mu_d = 200ms$.

Taking $\sigma_d^2 = 0$, we can plot P_{rev} against μ_d and σ_D, as shown in Figure 2.4.

2.3. The Platinum Pattern

Apart from the conventional blasting pattern discussed in the preceding section, various other blasting patterns are possible. Figure 2.5 gives a schematic representation of the blasting pattern used in platinum mines.

In this case, a reversal can occur in one of two ways, namely:

- If the maximum of D_{11} and D_{12} is larger than the aggregate delay time of D_2 and the minimum of d_{11} and d_{12}. Denote this by P_{rev}^{*1}.

- If D_2 is larger than the aggregate delay time of d_2 and the minimum of D_{31}

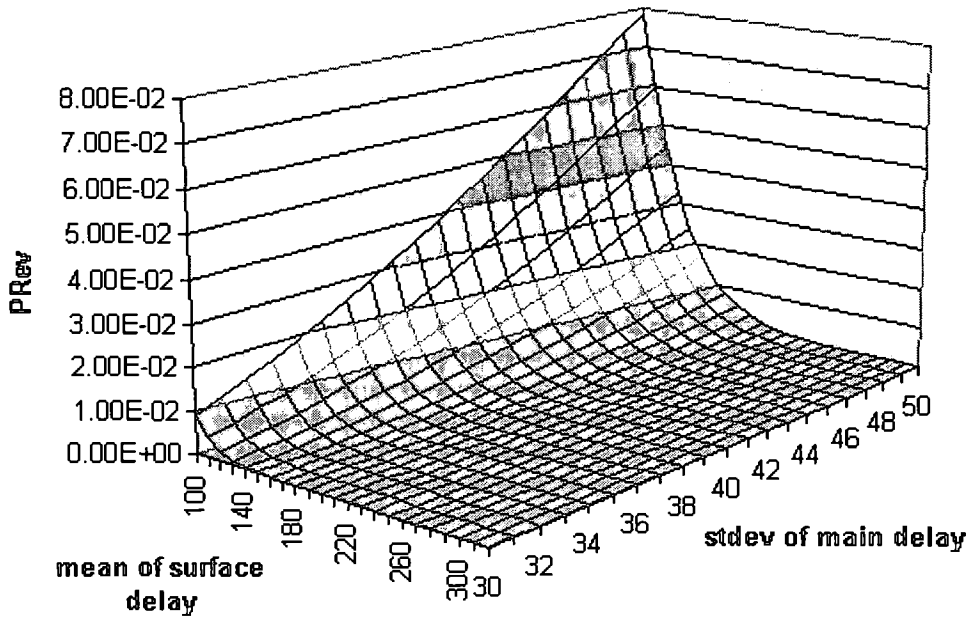

Figure 2.4: Pairwise probability of reversal, $\sigma_d = 0$.

and D_{32}. Denote this by P_{rev}^{*2}.

Consider first the case of a detonator pair in which a double main delay is followed by a single main delay. As before, assume that

$$\begin{aligned} D_{11}, D_{12}, D_2 &=_{\mathcal{L}} N(\mu_D, \sigma_D^2) \\ d_{11}, d_{12} &=_{\mathcal{L}} N(\mu_d, \sigma_d^2) \end{aligned} \quad . \tag{2.8}$$

Note that we can write $D_i = \mu_D + \sigma_D \cdot D_i^*$ and $d_i = \mu_d + \sigma_d \cdot d_i^*$, where D_i^*

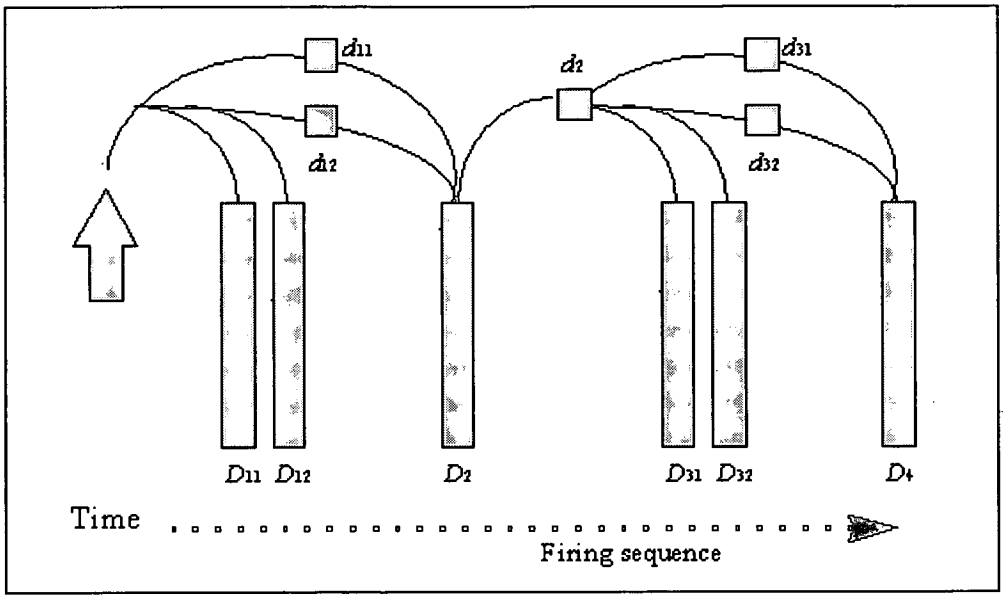

Figure 2.5: Schematic representation of platinum blasting pattern.

and d_i^* are standard $N(0,1)$ random variables. Then

$$\begin{aligned}
P_{rev}^{*1} &= P(\max(D_{11}, D_{12}) > D_2 + \min(d_{11}, d_{12})) \\
&= P(\max(D_{11} - D_2, D_{12} - D_2) > \min(d_{11}, d_{12})) \\
&= P(\max(\sigma_D(D_{11}^* - D_2^*), \sigma_D(D_{12}^* - D_2^*)) > \mu_d + \sigma_d \cdot \min(d_{11}^*, d_{12}^*)) \\
&= P(\max(\underbrace{D_{11}^* - D_2^*, D_{12}^* - D_2^*}_{\text{parameter free}}) > \tfrac{\mu_d}{\sigma_D} + \tfrac{\sigma_d}{\sigma_D} \cdot \min(\underbrace{d_{11}^*, d_{12}^*}_{\text{parameter free}})) \\
&= f(\tfrac{\mu_d}{\sigma_D}, \tfrac{\sigma_d}{\sigma_D}).
\end{aligned} \tag{2.9}$$

Similarly

$$\begin{aligned} P_{rev}^{*2} &= P(D_2 > d_2 + \min(D_{31}, D_{32})) \\ &= P(\min(D_{31} - D_2, D_{32} - D_2) < -d_2) \\ &= P(\min(\sigma_D(D_{31}^* - D_2^*), \sigma_D(D_{32}^* - D_2^*)) < -(\mu_d + \sigma_d \cdot d_2^*)) \\ &= P(\min(\underbrace{D_{31}^* - D_2^*, D_{32}^* - D_2^*}_{\text{parameter free}}) < -(\tfrac{\mu_d}{\sigma_D} + \tfrac{\sigma_d}{\sigma_D} \cdot d_2^*)) \\ &= g(\tfrac{\mu_d}{\sigma_D}, \tfrac{\sigma_d}{\sigma_D}). \end{aligned} \tag{2.10}$$

It is clear that μ_D, the mean of the main delays, does not feature in P_{rev}^{*1} and P_{rev}^{*2}, just as in the case of the standard gold pattern (see equation 2.4). Furthermore, if we make the reasonable approximation that $\sigma_d/\sigma_D = 0$, then

$$\begin{aligned} P_{rev}^{*1} &= P(\max(D_{11}^* - D_2^*, D_{12}^* - D_2^*) > \tfrac{\mu_d}{\sigma_D}) \\ &= E\left\{P(\max(D_{11}^* - D_2^*, D_{12}^* - D_2^*) > \tfrac{\mu_d}{\sigma_D}) \| D_2^*\right\} \\ &= 1 - E\left\{P(\max(\underbrace{D_{11}^* - D_2^*}_{N(-D_2^*,1)}, \underbrace{D_{12}^* - D_2^*}_{N(-D_2^*,1)}) \leq \tfrac{\mu_d}{\sigma_D}) \| D_2^*\right\} \\ &= 1 - E\left\{P(N(-D_2^*, 1) \leq \tfrac{\mu_d}{\sigma_D}) \cdot P(N(-D_2^*, 1) \leq \tfrac{\mu_d}{\sigma_D}) \| D_2^*\right\} \\ &= 1 - E\left\{\Phi^2(D_2^* + \tfrac{\mu_d}{\sigma_D}) \| D_2^*\right\} \\ &= 1 - \int \Phi^2(x + \tfrac{\mu_d}{\sigma_D}) \cdot \tfrac{1}{\sqrt{2\pi}} \exp(-\tfrac{x^2}{2}) \cdot dx \end{aligned} \tag{2.11}$$

and similarly

$$\begin{aligned} P_{rev}^{*2} &= P(\min(D_{31}^* - D_2^*, D_{32}^* - D_2^*) < -\tfrac{\mu_d}{\sigma_D}) \\ &= E\left\{P(\min(D_{31}^* - D_2^*, D_{32}^* - D_2^*) < -\tfrac{\mu_d}{\sigma_D}) \| D_2^*\right\} \\ &= E\left\{\Phi(D_2^* - \tfrac{\mu_d}{\sigma_D})\left(2 - \Phi(D_2^* - \tfrac{\mu_d}{\sigma_D})\right) \| D_2^*\right\} \\ &= \int \Phi(x - \tfrac{\mu_d}{\sigma_D})\left(2 - \Phi(x - \tfrac{\mu_d}{\sigma_D})\right) \cdot \tfrac{1}{\sqrt{2\pi}} \exp(-\tfrac{x^2}{2}) \cdot dx. \end{aligned} \tag{2.12}$$

2.4. Time series representation

Another way of looking at a reversal is in terms of a time series $\{T_1, T_2, \ldots, T_{n+1}\}$, with T_i defined as the instant at which the ith main delay explodes (measured from the instant at which the first main and surface delays were initiated). Then

$$T_i = \begin{cases} D_1 & ; i = 1 \\ d_1 + \ldots + d_{i-1} + D_i & ; 1 < i \leq n+1. \end{cases} \tag{2.13}$$

Example 1. *As an example of a possible outcome of such a time series, an observed sequence of five 4s main delays and four 0,25s surface delays in between might be the following:*

T_1	T_2	T_3	T_4	T_5
4,01	4,23	4,53	4,76	4,98

(2.14)

A series of k detonators will explode in sequence if and only if the following event occurs:

$$\{T_1 \leq T_2 \leq \ldots \leq T_k\}. \tag{2.15}$$

The event $R_i = \{A \textit{ reversal occurs at the } i\text{th } \textit{detonator pair}\}$ can also be expressed in terms of the variables T_i:

$$\begin{aligned} R_i &= \{T_{i+1} < T_i\} \\ &= \{T_{i+1} - T_i < 0\} \\ &= \{d_1 + d_2 + \ldots + d_{i-1} + d_i + D_{i+1} < d_1 + d_2 + \ldots + d_{i-1} + D_i\} \\ &= \{d_i + D_{i+1} < D_i\} \end{aligned} \tag{2.16}$$

which agrees with the representation used in (2.4).

It will be helpful in certain results that will follow later to also define a time series $\{Y_1, Y_2, \ldots, Y_n\}$, with

$$Y_i = T_{i+1} - T_i. \tag{2.17}$$

Y_i can be interpreted as the time that elapses between successive explosions, unless a reversal occurs. In terms of main and surface delay time distributions,

$$Y_i = d_i + D_{i+1} - D_i. \tag{2.18}$$

Note that Y_i will be negative if a reversal occurs in the ith detonator pair, since

$$\begin{aligned} & \{Y_i < 0\} \\ = \; & \{d_i + D_{i+1} - D_i < 0\} \\ = \; & \{d_i + D_{i+1} < D_i\} \\ = \; & R_i. \end{aligned} \tag{2.19}$$

Furthermore

$$\begin{aligned} E(Y_i) &= E(d_i + D_{i+1} - D_i) \\ &= \mu_d. \end{aligned} \tag{2.20}$$

and

$$\begin{aligned} var(Y_i) &= var(d_i + D_{i+1} - D_i) \\ &= 2\sigma_D^2 + \sigma_d^2. \end{aligned} \tag{2.21}$$

Therefore

$$Y_i =_{\mathcal{L}} N(\mu_d, 2\sigma_D^2 + \sigma_d^2). \tag{2.22}$$

Note that successive random variables Y_i and Y_{i+1} are not independent, since

$$\begin{aligned} cov(Y_i, Y_{i+1}) &= cov(d_i + D_{i+1} - D_i, d_{i+1} + D_{i+2} - D_{i+1}) \\ &= -var(D_{i+1}) \\ &= -\sigma_D^2. \end{aligned} \tag{2.23}$$

$$\begin{aligned} \rho(Y_i, Y_{i+1}) &= \frac{cov(Y_i, Y_{i+1})}{2\sigma_D^2 + \sigma_d^2} \\ &= \frac{-\sigma_D^2}{2\sigma_D^2 + \sigma_d^2} \\ &= -\frac{1}{2 + \left(\sigma_d^2/\sigma_D^2\right)} \\ &\approx -\frac{1}{2} \end{aligned}$$

Since Y_i and Y_j, with $j - i > 1$, share no common components, it is easy to see that

$$\rho(Y_i, Y_j) = 0 \qquad ; j - i > 1. \tag{2.24}$$

The successive time periods between explosions are therefore negatively correlated, while the times between explosions of non-adjacent pairs of detonators are uncorrelated, and therefore (since they are normal variables) independent.

2.5. Evaluating $P(R)$

The pairwise probability of reversal P_{rev}, while theoretically useful, is not of much use in practice. The major concern of end-users of detonators (and therefore also

their suppliers!) is the probability of a sequence of $n+1$ main delays and n surface delays failing somewhere along the line, i.e. the probability of a reversal occurring in one or more of the individual pairs that make up the blasting sequence. If we denote this probability by $P(R)$, we want

$$P(R) = P(\cup_{i=1}^{n} R_i). \tag{2.25}$$

However, the events $R_1, R_2, \ldots, R_n$ are not mutually exclusive, so that $P(R)$ cannot be obtained simply by summing the $P(R_i)$. Consider the following standard result of probability theory in the case of two events R_1 and R_2:

$$P(R_1 \cup R_2) = P(R_1) + P(R_2) - P(R_1 \cap R_2). \tag{2.26}$$

This can be expanded to three events as follows:

$$P(R_1 \cup R_2 \cup R_3) = \left(\begin{array}{l} P(R_1) + P(R_2) + P(R_3) \\ -P(R_1 \cap R_2) - P(R_1 \cap R_3) - P(R_2 \cap R_3) \\ +P(R_1 \cap R_2 \cap R_3). \end{array} \right) \tag{2.27}$$

In general,

$$P(\cup_{i=1}^{n} R_i) = \left(\begin{array}{l} \sum_{i=1}^{n} P(R_i) \\ -\sum_{i=1}^{n-1} \sum_{j=i+1}^{n} P(R_i \cap R_j) \\ +\sum_{i=1}^{n-2} \sum_{j=i+1}^{n-1} \sum_{k=j+1}^{n} P(R_i \cap R_j \cap R_k) \\ \quad \vdots \\ +(-1)^{n-1} P(\cap_{i=1}^{n} R_i). \end{array} \right) \tag{2.28}$$

(see Feller (1968), pp. 98-111, for further details).

It will be convenient to define a series of partial sums $S_1, S_2, \ldots, S_n$ such that

$$S_i = \sum (\text{first } i \text{ terms of (2.28)}), \tag{2.29}$$

i.e.

$$\begin{aligned} S_1 &= \textstyle\sum_{i=1}^{n} P(R_i) \\ S_2 &= S_1 - \textstyle\sum_{i=1}^{n-1} \sum_{j=i+1}^{n} P(R_i \cap R_j) \\ S_3 &= S_2 + \textstyle\sum_{i=1}^{n-2} \sum_{j=i+1}^{n-1} \sum_{k=j+1}^{n} P(R_i \cap R_j \cap R_k) \\ &\vdots \\ S_k &= S_{k-1} + \Theta_k \\ &\vdots \\ S_n &= S_{n-1} + (-1)^{n-1} P(\cap_{i=1}^{n} R_i) \end{aligned} \tag{2.30}$$

where

$$\begin{aligned} \Theta_k &= (-1)^{k-1} \prod_{\gamma=1}^{k} \sum_{\beta_\gamma=\beta_{\gamma-1}+1}^{n-k+\gamma} P\left(\bigcap_{\delta=1}^{k} R_{\beta_\delta}\right) \\ \beta_0 &= 0. \end{aligned} \tag{2.31}$$

Note that the terms of (2.28) alternate in sign. The absolute error when truncating the sum after the ith term is therefore less than or equal to the absolute value of term $i+1$, i.e.

$$|S_n - S_i| \leq |\Theta_{i+1}| . \tag{2.32}$$

As a first step, therefore, we can state an upper bound for $P(R)$ by ignoring all terms following the first, i.e.

$$P(\cup_{i=1}^{n} R_i) \leq S_1 = \sum_{i=1}^{n} P(R_i) = n \cdot \Phi(\lambda) . \tag{2.33}$$

This is known as *Boole's Inequality.* Similarly we can develop a lower bound by retaining the first two terms, i.e.

$$P(\cup_{i=1}^{n} R_i) \geq S_2 = \sum_{i=1}^{n} P(R_i) - \sum_{i=1}^{n-1} \sum_{j=i+1}^{n} P(R_i \cap R_j). \tag{2.34}$$

In this way $P(R)$ can be calculated to any required degree of accuracy ε by merely considering the partial sums S_i until $S_i - S_{i-1} < \varepsilon$. However, in attempting to evaluate terms such as $P(R_i \cap R_j)$ one should keep in mind that R_i and R_j are usually, but not always, statistically independent. To see this, consider the

following three events:

Event	*Description*	*Happens if*
R_5	Reversal of 5th pair	$d_5 + D_6 < D_5$
R_6	Reversal of 6th pair	$d_6 + D_7 < D_6$
R_7	Reversal of 7th pair	$d_7 + D_8 < D_7$

(2.35)

Now note that R_5 and R_6 share the same component D_6 and can therefore not be independent. R_5 and R_7, however, have no components in common, and since the individual components are independent by assumption, the composite events R_5 and R_7 are also independent.

This holds in general, i.e. two pairwise reversal events R_α and R_β are

$$\begin{cases} \text{dependent} & \text{if } |\alpha - \beta| < 2 \\ \text{independent} & \text{if } |\alpha - \beta| \geq 2 \end{cases} \tag{2.36}$$

(2.36) can also be seen by considering the time series representation of the times between explosions, as introduced in (2.13) and (2.17). Recall that

$$\{R_\alpha\} \Longleftrightarrow \{Y_\alpha < 0\}. \tag{2.37}$$

Successive Y_α and $Y_{\alpha+1}$ are negatively correlated, while Y_α and Y_β are uncorrelated

and independent when $|\alpha - \beta| \geq 2$ (see (2.23) and (2.24)).

The second term in (2.28), $\sum_{i=1}^{n-1} \sum_{j=i+1}^{n} P(R_i \cap R_j)$, consists of a number of terms of the form

$$\begin{bmatrix} 1,2 & 1,3 & 1,4 & \dots & 1,n-1 & 1,n \\ & 2,3 & 2,4 & \dots & 2,n-1 & 2,n \\ & & 3,4 & \dots & 3,n-1 & 3,n \\ & & & \ddots & \vdots & \vdots \\ & & & & (n-2),(n-1) & (n-2),n \\ & & & & & (n-1),n \end{bmatrix} \tag{2.38}$$

where a pair i, j denotes $P(R_i \cap R_j)$. Note that the terms on the diagonal are of the form $P(R_i \cap R_{i+1}) = P(R_1 \cap R_2)$, while the other terms are all equal to

$$\begin{aligned} P(R_i \cap R_j) &= P(R_i) \cdot P(R_j) \qquad ; j - i > 1 \\ &= \Phi^2(\lambda). \end{aligned} \tag{2.39}$$

(2.38) then becomes

$$\begin{bmatrix} P(R_1 \cap R_2) & \Phi^2(\lambda) & \Phi^2(\lambda) & \dots & \Phi^2(\lambda) & \Phi^2(\lambda) \\ & P(R_1 \cap R_2) & \Phi^2(\lambda) & \dots & \Phi^2(\lambda) & \Phi^2(\lambda) \\ & & P(R_1 \cap R_2) & \dots & \Phi^2(\lambda) & \Phi^2(\lambda) \\ & & & \ddots & \vdots & \vdots \\ & & & & P(R_1 \cap R_2) & \Phi^2(\lambda) \\ & & & & & P(R_1 \cap R_2) \end{bmatrix}_{(n-1)\times(n-1)} \tag{2.40}$$

It can be shown that

$$\begin{aligned} P(R_1 \cap R_2) &= P\left(d_1 + D_2 < D_1 \text{ and } d_2 + D_3 < D_2\right) \\ &= E\left\{\Phi\left(\tfrac{D_2-\mu_d+\mu_D}{\sqrt{\sigma_D^2+\sigma_d^2}}\right) \cdot \Phi\left(\tfrac{D_2-\mu_d-\mu_D}{\sqrt{\sigma_D^2+\sigma_d^2}}\right) \| D_2\right\} \\ &= \int \Phi\left(\tfrac{x-\mu_d+\mu_D}{\sqrt{\sigma_D^2+\sigma_d^2}}\right) \cdot \Phi\left(\tfrac{x-\mu_d-\mu_D}{\sqrt{\sigma_D^2+\sigma_d^2}}\right) \cdot \tfrac{1}{\sqrt{2\pi}\sigma_D} \exp\left(\tfrac{-(x-\mu_D)^2}{2\sigma_D^2}\right) dx \end{aligned} \tag{2.41}$$

and, similarly,

$$\begin{aligned} & P(R_1 \cap R_2 \cap R_3) \\ = \; & P\left(d_1 + D_2 < D_1 \text{ and } d_2 + D_3 < D_2 \text{ and } d_3 + D_4 < D_3\right) \\ = \; & E\left[E\left\{\Phi\left(\tfrac{D_2-\mu_d+\mu_D}{\sqrt{\sigma_D^2+\sigma_d^2}}\right) \Phi\left(\tfrac{D_2-D_3-\mu_d}{\sigma_d}\right) \Phi\left(\tfrac{D_3-\mu_d-\mu_D}{\sqrt{\sigma_D^2+\sigma_d^2}}\right) \| D_2, D_3\right\}\right] \\ = \; & \int\int \Phi\left(\tfrac{x-\mu_d+\mu_D}{\sqrt{\sigma_D^2+\sigma_d^2}}\right) \Phi\left(\tfrac{x-y-\mu_d}{\sigma_d}\right) \Phi\left(\tfrac{y-\mu_d-\mu_D}{\sqrt{\sigma_D^2+\sigma_d^2}}\right) \cdot \tfrac{1}{2\pi\sigma_D^2} \exp\left(\tfrac{-(x-\mu_D)^2-(y-\mu_D)^2}{2\sigma_D^2}\right) dxdy. \end{aligned} \tag{2.42}$$

These functions can be evaluated using numerical integration, simulation or other similar numerical techniques, to be used in calculating $P(R)$ exactly. This results in negligible improvements in accuracy, though, since in practice

$$\begin{aligned} P(R_1 \cap R_2) &\ll P(R_i \cap R_j) \\ P(R_1 \cap R_2 \cap R_3) &\ll P(R_i \cap R_j \cap R_k) \\ \vdots &\ll \vdots \end{aligned} \tag{2.43}$$

and in fact, probabilities of the form $P(R_1 \cap R_2 \cap \ldots)$ are so small that they can be taken as 0.

To see this, consider the event

$$\begin{aligned} P(R_1 \cap R_2) &= P(d_1 + D_2 < D_1 \text{ and } d_2 + D_3 < D_2) \\ &= P\left(\underbrace{d_2 + D_3}_{N(\mu_D+\mu_d,\sigma_D^2+\sigma_d^2)} < \underbrace{D_2}_{N(\mu_D,\sigma_D^2)} < \underbrace{D_1 - d_1}_{N(\mu_D-\mu_d,\sigma_D^2+\sigma_d^2)} \right). \end{aligned} \tag{2.44}$$

Figure 2.6 depicts the three distributions described in (2.44) for a typical case in practice where $\mu_D = 3800, \mu_d = 200, \sigma_D = 40$ and $\sigma_d = 5$, i.e.

$$\begin{aligned} D_2 :=& \quad X_1 =_{\mathcal{L}} N(3800, 40^2) \\ D_1 - d_1 :=& \quad X_2 =_{\mathcal{L}} N(3600, 40^2 + 5^2) \\ d_2 + D_3 :=& \quad X_3 =_{\mathcal{L}} N(4000, 40^2 + 5^2) \end{aligned} \tag{2.45}$$

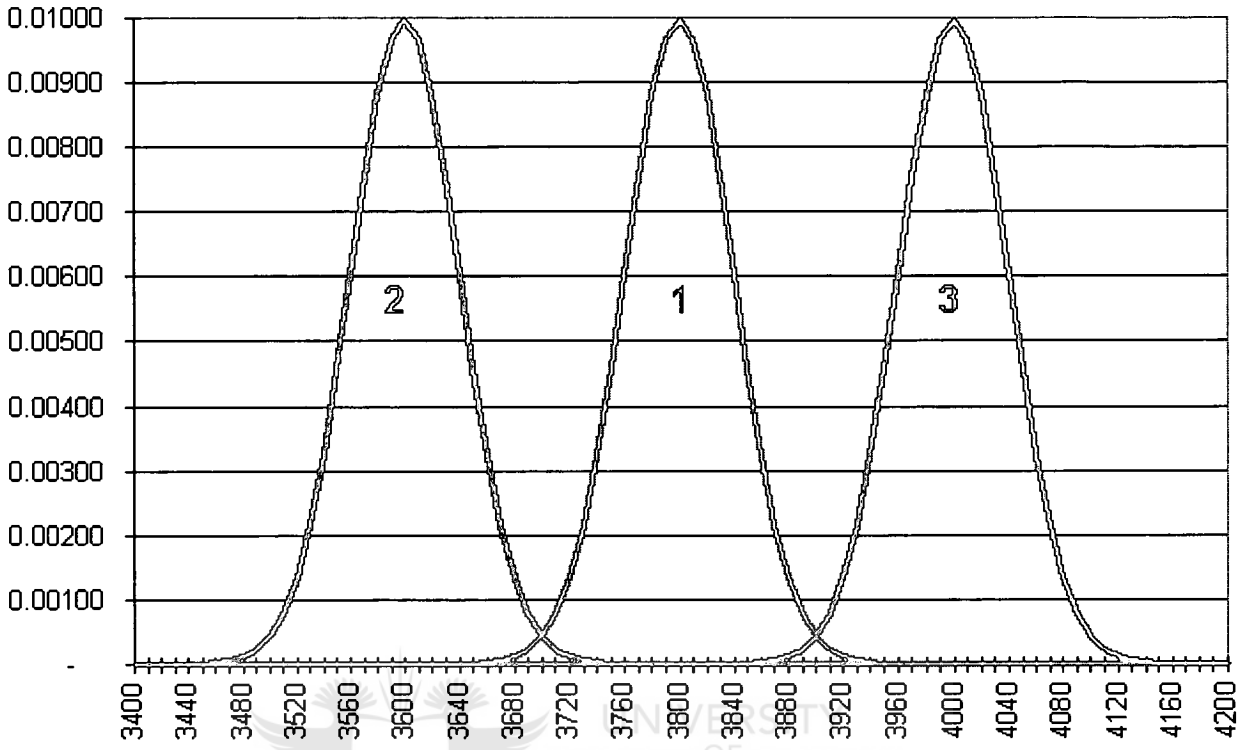

Figure 2.6: $N(3800, 40^2), N(3800 \pm 200, 40^2 + 5^2)$ density functions.

The event $\{R_1 \cap R_2\}$ is equivalent to sampling three values x_1, x_2 and x_3 from the three distributions X_1, X_2 and X_3 (labelled 1, 2 and 3 respectively on Figure 2.6) and requiring that $x_3 < x_1 < x_2$. A less stringent requirement will be that $x_3 < x_2$, which, from Figure 2.6, still seems highly unlikely. The distance between the means of X_2 and X_3 is $4000 - 3600 = 400$, almost **ten times** their common standard deviation of $\sqrt{40^2 + 5^2} = 40,3$.

Another way of investigating the behaviour of $P(R_1 \cap R_2)$ is to consider the

alternative time series representation introduced in (2.13) and (2.17). Clearly,

$$P(R_1 \cap R_2) = P(Y_1 < 0 \text{ and } Y_2 < 0) \cdot \tag{2.46}$$

From (2.23), however, Y_1 and Y_2 are **negatively** correlated, implying that below average times between explosions (probable reversals) are generally immediately followed by above average times (i.e. probable non-reversals). It would therefore seem reasonable to expect that $P(R_1 \cap R_2)$ will be much less than $P(R_i \cap R_j) = \Phi^2(\lambda)$ for $j - i > 1$.

This can be confirmed by comparing the bivariate normal distribution of the pair (Y_1, Y_2) with the joint distribution of (Y_i, Y_j) with $j - i > 1$. The joint density function of Y_1 and Y_2 is

$$f(y_1, y_2) = \frac{1}{2\pi\sigma^2\sqrt{1-\rho^2}} \exp \frac{-1}{2\sigma^2(1-\rho^2)} \left((y_1-\mu)^2 - 2\rho(y_1-\mu)(y_2-\mu) + (y_2-\mu)^2\right) \tag{2.47}$$

where, from (2.20) and (2.23),

$$\begin{aligned} \mu &= \mu_d \\ \sigma^2 &= 2\sigma_D^2 + \sigma_d^2 \\ \rho &= \frac{-\sigma_D^2}{2\sigma_D^2+\sigma_d^2} \approx -\frac{1}{2}. \end{aligned} \tag{2.48}$$

Therefore

$$P(Y_i < 0, Y_{i+1} < 0) = \int_{-\infty}^{0}\int_{-\infty}^{0} f(y_1, y_2) \cdot dy_1 dy_2. \tag{2.49}$$

Change variables by setting

$$\frac{y_i - \mu}{\sigma} = y_i^*, \qquad i = 1, 2 \tag{2.50}$$

in (2.47). Then the joint density function of y_1^* and y_2^* is

$$g(y_1^*, y_2^*) = \frac{1}{2\pi\sigma^2\sqrt{1-\rho^2}} \exp \frac{-1}{2(1-\rho^2)} \left(y_1^{*2} - 2\rho y_1^* y_2^* + y_2^{*2}\right). \tag{2.51}$$

In this case the integration region $(-\infty, 0] \times (-\infty, 0]$ of (2.49) becomes

$$\begin{aligned} & (-\infty, \tfrac{-\mu}{\sigma}] \times (-\infty, \tfrac{-\mu}{\sigma}] \\ = \; & (-\infty, -\xi] \times (-\infty, -\xi], \text{ say.} \end{aligned} \tag{2.52}$$

Now consider the difference between the joint density function of an independent pair of random variables (Y_i, Y_j), $j - i > 0$ and that of a dependent pair (Y_1, Y_2). This implies considering $\rho = 0$ against the alternative $\rho \approx -\frac{1}{2}$ (from (2.48)). We can examine the logarithms of the two density functions, since we are

only interested in the sign of the difference over the area $(-\infty, -\xi] \times (-\infty, -\xi]$.

$$\begin{aligned} & \log g(y_1^*, y_2^*)_{\rho=0} - \log g(y_1^*, y_2^*)_{\rho=-\frac{1}{2}} \\ = & -\tfrac{1}{2}\left(y_1^{*2} + y_2^{*2}\right) + \tfrac{1}{2}\log\left(\tfrac{3}{4}\right) + \tfrac{2}{3}\left(y_1^{*2} + y_1^* y_2^* + y_2^{*2}\right) \\ = & \tfrac{1}{6}\left(y_1^{*2} + 4y_1^* y_2^* + y_2^{*2}\right) + \tfrac{1}{2}\log\left(\tfrac{3}{4}\right) \\ > & \tfrac{1}{6}\left(\xi^2 + 4\xi^2 + \xi^2\right) + \tfrac{1}{2}\log\left(\tfrac{3}{4}\right) \qquad \forall \quad y_1^*, y_2^* < -\xi \\ = & \xi^2 - 0,144. \end{aligned} \tag{2.53}$$

This indicates that

- the joint density function of (Y_i, Y_j), $j - i > 1$, is **pointwise greater than** the density function of (Y_1, Y_2) over the area $(-\infty, -\xi] \times (-\infty, -\xi]$ as long as

$$\xi > \sqrt{0,144} = 0,37. \tag{2.54}$$

(2.54) holds in practice, because

$$\xi = \frac{\mu}{\sigma} = \frac{\mu_d}{\sqrt{2\sigma_D^2 + \sigma_d^2}} \gg 1. \tag{2.55}$$

Therefore

$$\begin{aligned} \int_{-\infty}^{-\xi}\int_{-\infty}^{-\xi} g(y_1^*, y_2^*)_{\rho=-1/2} dy_1^* dy_2^* & < \int_{-\infty}^{-\xi}\int_{-\infty}^{-\xi} g(y_1^*, y_2^*)_{\rho=0} dy_1^* dy_2^* \\ \Rightarrow \qquad P(R_1 \cap R_2) & < P(R_i \cap R_j) = \Phi^2(\lambda). \end{aligned} \tag{2.56}$$

We can now obtain a very good approximation for $P(R)$ by calculating S_n, but ignoring terms of the form $P(R_1 \cap R_2)$ and any combinations thereof, such as $P(R_1 \cap R_2 \cap R_5)$ or $P(R_1 \cap R_4 \cap R_5)$.

$$\begin{aligned} P(R) &= \textstyle\sum_{i=1}^{n} P(R_i) - \sum_{i=1}^{n-1} \sum_{j=i+1}^{n} P(R_i \cap R_j) + \ldots \\ &\approx n\Phi(\lambda) - \tfrac{(n-2)(n-1)}{2}\Phi^2(\lambda) + \tfrac{(n-4)(n-3)(n-2)}{6}\Phi^3(\lambda) - \ldots \\ &= \tbinom{n}{1}\Phi(\lambda) - \tbinom{n-1}{2}\Phi^2(\lambda) + \tbinom{n-2}{3}\Phi^3(\lambda) - \ldots \\ &= \sum_{i=1}^{\lfloor (n+1)/2 \rfloor} (-1)^{i-1}\tbinom{n-i+1}{i}\Phi^i(\lambda). \end{aligned} \tag{2.57}$$

The following Matlab m-file will calculate $P(R)$ for given parameters n, μ_d, σ_d and σ_D:


```
function output = pr(n,mu_d,s_main,s_surf)
%function output = pr(n,mu_d,s_main,s_surf)
lambda=-mu_d/(s_surf^2+2*s_main^2)^0.5;
phi=normcdf(lambda);
terms=floor((n+1)/2);
phiMat=phi.^[1:terms]';
for i=1:terms;
 comb(1,i)=(-1)^(i-1)*prod(n-2*i+2:n-i+1)/prod(1:i);
end;
output=comb*phiMat;
```

The m-function above calculates the first x terms of (2.57) very efficiently

using matrix multiplication, since

$$= \begin{bmatrix} \sum_{i=1}^{\lfloor (n+1)/2 \rfloor} (-1)^{i-1} \binom{n-i+1}{i} \Phi^i(\lambda) \\ n \\ -(2!)^{-1}(n-2)(n-1) \\ (3!)^{-1}(n-4)(n-3)(n-2) \\ \vdots \\ (-1)^{i-1}\binom{n-i+1}{i} \\ \vdots \end{bmatrix}' \times \begin{bmatrix} \Phi(\lambda) \\ \Phi^2(\lambda) \\ \Phi^3(\lambda) \\ \vdots \\ \Phi^i(\lambda) \\ \vdots \end{bmatrix}. \tag{2.58}$$

2.6. Estimating $P(R)$

In the preceding section we saw how $P(R)$ can be calculated when the parameters μ_d, σ_D^2, σ_d^2 and n are known. Apart from n, these parameters are usually unknown and they will therefore have to be estimated.

Suppose that s samples of surface delays and m samples of main delays are available for analysis. Denote these samples by $d_1, d_2, \ldots, d_s$ and $D_1, D_2, \ldots, D_m$ respectively. From these samples it is possible to compute unbiased estimators of

μ_D, σ_d^2 and σ_D^2, namely

$$\begin{aligned} \hat{\mu}_d &= \bar{d}, \text{ the sample mean of } d_1, d_2, \ldots, d_s \\ \hat{\sigma}_d^2 &= S_d^2 = \tfrac{1}{s-1}\textstyle\sum_{i=1}^{s}(d_i - \bar{d})^2 \\ \hat{\sigma}_D^2 &= S_D^2 = \tfrac{1}{m-1}\textstyle\sum_{i=1}^{m}(D_i - \bar{D})^2. \end{aligned} \tag{2.59}$$

An obvious estimator for $P_{rev} = \Phi(\lambda)$, for example, is

$$\begin{aligned} \widehat{P_{rev}} &= \Phi\left(\tfrac{-\hat{\mu}_d}{\sqrt{\hat{\sigma}_d^2 + 2\hat{\sigma}_D^2}}\right) \\ &= \Phi\left(\tfrac{-\bar{d}}{\sqrt{S_d^2 + 2S_D^2}}\right) \\ &= \Phi(\hat{\lambda}) \end{aligned} \tag{2.60}$$

and this in turn can be used in (2.57) to estimate $P(R)$, i.e.

$$\widehat{P(R)} = \sum_{i=1}^{\lfloor (n+1)/2 \rfloor} (-1)^{i-1} \binom{n-i+1}{i} \Phi^i(\hat{\lambda}). \tag{2.61}$$

While the estimators $\bar{d}$, S_d^2 and S_D^2 are unbiased, $\widehat{P_{rev}}$ and $\widehat{P(R)}$, being highly nonlinear functions of these, can be expected to be biased, perhaps severely so.

2.7. Bias considerations

2.7.1. The bias of $\hat{\lambda}$

As a first step we could investigate the bias in $\hat{\lambda}$ under the simplifying (and not unreasonable) assumption that $\sigma_d^2 = 0$. In this case $\hat{\mu}_d = \mu_d$ and

$$\begin{aligned} \hat{\lambda} &= \frac{-\mu_d}{\sqrt{2\hat{\sigma}_D^2}} \\ &= f(\hat{\sigma}_D^2). \end{aligned} \tag{2.62}$$

Using the Taylor series expansion

$$\begin{aligned} \underbrace{f(\hat{\sigma}_D^2)}_{\hat{\lambda}} &\approx f(\sigma_D^2) + (\hat{\sigma}_D^2 - \sigma_D^2)\frac{df}{d\sigma_D^2} + \tfrac{1}{2}(\hat{\sigma}_D^2 - \sigma_D^2)^2 \frac{d^2 f}{d\left(\sigma_D^2\right)^2} \\ &= f(\sigma_D^2) + (\hat{\sigma}_D^2 - \sigma_D^2)\frac{d}{d\sigma_D^2}\left(\frac{-\mu_d}{\sqrt{2\sigma_D^2}}\right) + \tfrac{1}{2}(\hat{\sigma}_D^2 - \sigma_D^2)^2 \frac{d^2}{d\left(\sigma_D^2\right)^2}\left(\frac{-\mu_d}{\sqrt{2\sigma_D^2}}\right) \\ &= \underbrace{f(\sigma_D^2)}_{\lambda} + (\hat{\sigma}_D^2 - \sigma_D^2)\frac{\mu_d}{2\sqrt{2}\left(\sigma_D^2\right)^{3/2}} + \tfrac{1}{2}(\hat{\sigma}_D^2 - \sigma_D^2)^2 \frac{-3\mu_d}{4\sqrt{2}\left(\sigma_D^2\right)^{5/2}} \end{aligned} \tag{2.63}$$

Therefore

$$\begin{aligned} E(\hat{\lambda} - \lambda) &\approx E\left((\hat{\sigma}_D^2 - \sigma_D^2)\frac{\mu_d}{2\sqrt{2}\left(\sigma_D^2\right)^{3/2}} + \tfrac{1}{2}(\hat{\sigma}_D^2 - \sigma_D^2)^2 \frac{-3\mu_d}{4\sqrt{2}\left(\sigma_D^2\right)^{5/2}}\right) \\ &= 0 + var(S_D^2) \cdot \tfrac{1}{2} \cdot \frac{-3\mu_d}{4\sqrt{2}\left(\sigma_D^2\right)^{5/2}} \\ &= \frac{2\sigma_D^4}{n-1} \cdot \tfrac{1}{2} \cdot \frac{-3\mu_d}{4\sqrt{2}\left(\sigma_D^2\right)^{5/2}} \\ &= \frac{-3\mu_d}{4(n-1)\sqrt{2}\sigma_D} \\ &= \frac{3}{4(n-1)}\lambda. \end{aligned} \tag{2.64}$$

From (2.64) it is clear that the bias in $\hat{\lambda}$ is of the same order as λ, but decreasing as the sample size n increases.

2.7.2. The bias of $\widehat{P_{rev}}$

To investigate the bias that might be present in $\widehat{P_{rev}}$, a Monte Carlo study is most helpful. For the purposes of this simulation, the following parameters were chosen *a priori* to represent the true underlying distributions of the d_i and D_i:

$$\begin{aligned} \mu_d &= 200 \\ \sigma_d^2 &= 4^2, 6^2, 8^2 \\ \sigma_D^2 &= 40^2, 50^2, 60^2. \end{aligned} \tag{2.65}$$

Given these underlying parameters, the true probabilities of reversal can be calculated as

	$\sigma_d = 4$	$\sigma_d = 6$	$\sigma_d = 8$
$\sigma_D = 40$	$2,1036 \times 10^{-4}$	$2,1921 \times 10^{-4}$	$2,3202 \times 10^{-4}$
$\sigma_D = 50$	$2,3721 \times 10^{-3}$	$2,4139 \times 10^{-3}$	$2,4733 \times 10^{-3}$
$\sigma_D = 60$	$9,2761 \times 10^{-3}$	$9,3577 \times 10^{-3}$	$9,4724 \times 10^{-3}$

(2.66)

Two sample sizes were investigated, namely $s = m = 25$ and $s = m = 50$. In each case 1000 samples from the relevant distributions were simulated and $\widehat{P_{rev}}$

was calculated for each sample and then averaged. The following tables show the estimated $E(\widehat{P_{rev}})$ and its relative bias, $\frac{\hat{E}(\widehat{P_{rev}})-P_{rev}}{P_{rev}}$ (in brackets), for the two sample sizes:

$\mathbf{s = m = 25}$	$\sigma_d = 4$	$\sigma_d = 6$	$\sigma_d = 8$
$\sigma_D = 40$	$5,1541 \times 10^{-4}$ $(1,4501)$	$5,2902 \times 10^{-4}$ $(1,4133)$	$5,4830 \times 10^{-4}$ $(1,3632)$
$\sigma_D = 50$	$3,4378 \times 10^{-3}$ $(0,4493)$	$3,4841 \times 10^{-3}$ $(0,4433)$	$3,5487 \times 10^{-3}$ $(0,4348)$
$\sigma_D = 60$	$1,0866 \times 10^{-2}$ $(0,1713)$	$1,0949 \times 10^{-2}$ $(0,1700)$	$1,1064 \times 10^{-2}$ $(0,1681)$

(2.67)

and

$\mathbf{s = m = 50}$	$\sigma_d = 4$	$\sigma_d = 6$	$\sigma_d = 8$
$\sigma_D = 40$	$3,5608 \times 10^{-4}$ $(0,6927)$	$3,6708 \times 10^{-4}$ $(0,6746)$	$3,8289 \times 10^{-4}$ $(0,6503)$
$\sigma_D = 50$	$2,9054 \times 10^{-3}$ $(0,2248)$	$2,9477 \times 10^{-3}$ $(0,2211)$	$3,0077 \times 10^{-3}$ $(0,2161)$
$\sigma_D = 60$	$1,0052 \times 10^{-2}$ $(0,0837)$	$1,0130 \times 10^{-2}$ $(0,0825)$	$1,0240 \times 10^{-2}$ $(0,0811)$

(2.68)

The pattern is clear — the relative bias of $\widehat{P_{rev}}$ **decreases** in line with **increases** in σ_d, σ_D and sample size.

2.7.3. The bias of $\widehat{P(R)}$

Given the parameters as shown in (2.65), the true $P(R)$ for a sequence of 20 detonator pairs can be calculated as

	$\sigma_d = 4$	$\sigma_d = 6$	$\sigma_d = 8$
$\sigma_D = 40$	$4,1997 \times 10^{-3}$	$4,3759 \times 10^{-3}$	$4,6312 \times 10^{-3}$
$\sigma_D = 50$	$4,6490 \times 10^{-2}$	$4,7294 \times 10^{-2}$	$4,8431 \times 10^{-2}$
$\sigma_D = 60$	$1,7144 \times 10^{-1}$	$1,7283 \times 10^{-1}$	$1,7478 \times 10^{-1}$

(2.69)

Once again I employed Monte Carlo studies to obtain estimates for the bias in $\widehat{P(R)}$, using the unbiased estimates given in (2.59) as the parameters for (2.61).

The estimated $E(\widehat{P(R)})$ and its relative bias are detailed in the following tables.

$\mathbf{s = m = 25}$	$\sigma_d = 4$	$\sigma_d = 6$	$\sigma_d = 8$
$\sigma_D = 40$	$9,6540 \times 10^{-3}$ $(1,2992)$	$9,8837 \times 10^{-3}$ $(1,2591)$	$1,0218 \times 10^{-2}$ $(1,2068)$
$\sigma_D = 50$	$6,2165 \times 10^{-2}$ $(0,3401)$	$6,2880 \times 10^{-2}$ $(0,3325)$	$6,3909 \times 10^{-2}$ $(0,3226)$
$\sigma_D = 60$	$1,8146 \times 10^{-1}$ $(0,0671)$	$1,8254 \times 10^{-1}$ $(0,0649)$	$1,8411 \times 10^{-1}$ $(0,0622)$

(2.70)

and

$\mathbf{s = m = 50}$	$\sigma_d = 4$	$\sigma_d = 6$	$\sigma_d = 8$
$\sigma_D = 40$	$7,3668 \times 10^{-3}$ $(0,7545)$	$7,5844 \times 10^{-3}$ $(0,7336)$	$7,8971 \times 10^{-3}$ $(0,7056)$
$\sigma_D = 50$	$5,6293 \times 10^{-2}$ $(0,2135)$	$5,7080 \times 10^{-2}$ $(0,2096)$	$5,8190 \times 10^{-2}$ $(0,2043)$
$\sigma_D = 60$	$1,7804 \times 10^{-1}$ $(0,0470)$	$1,7932 \times 10^{-1}$ $(0,0461)$	$1,8110 \times 10^{-1}$ $(0,0448)$

(2.71)

It can be seen that the relative bias in $\widehat{P(R)}$ is less than that of $\widehat{P_{rev}}$. As was the case with $\widehat{P_{rev}}$, the relative bias in $\widehat{P(R)}$ also **decreases** in line with **increases**

in σ_d, σ_D and sample size. This is not too surprising since $P(R)$ is a mostly linear function of P_{rev}, i.e.

$$P(R) \approx nP_{rev}. \tag{2.72}$$

Any technique that results in a reduction of the bias in $\widehat{P_{rev}}$ will also benefit $\widehat{P(R)}$. This is the subject of the next section.

2.8. Reducing the bias of $\widehat{P_{rev}}$

One method of reducing the bias of $\widehat{P_{rev}} = \Phi(\hat{\lambda})$ is the *jackknife*, a general technique for reducing bias in a point-estimator (see Quenouille (1956) and Miller (1974) for further discussions of the technique and its properties). The one-sample jackknife is defined as follows. Let

$$X_1, X_2, \ldots, X_n \tag{2.73}$$

be a random sample, and let

$$T_n = T_n(X_1, X_2, \ldots, X_n) \tag{2.74}$$

be some estimator of a parameter θ. Define n statistics $T_n^{(i)}$, $i = 1, \ldots, n$, where $T_n^{(i)}$ is calculated just as T_n except that the value X_i is removed from the sample.

The jackknife estimator of θ is then given by

$$JK(T_n) = nT_n - \frac{n-1}{n}\sum_{i=1}^{n} T_n^{(i)}. \tag{2.75}$$

I shall use this technique on a sample of main delay data and given (or estimated) μ_d and σ_d. One could refine this further by using the two-sample variation of the jackknife on both main and surface delay samples, but the added reduction in bias from the surface delay data is small.

The following Matlab m-function calculates the Jackknife estimators of P_{rev} for a random sample or number of samples of surface delay data, given μ_d and σ_d.


```
function output = jkprev(X, mu_s, sigma_s)
%function output = jkprev(X, mu_s, sigma_s)
%Calculates the jackknife estimators of PRev from data X.
[r,c]=size(X);
Tn=normcdf(-mu_s./sqrt(sigma_s^2+2*var(X)));
Tstats=normcdf(-mu_s./sqrt(sigma_s^2+2*var(X(2:r,:))));
for i=2:r;
 redVar=var([X(1:(i-1),:);X((i+1):r,:)]);
 redPhiHat=normcdf(-mu_s./sqrt(sigma_s^2+2*redVar));
 Tstats=[Tstats;redPhiHat];
end;
JK=r*Tn-((r-1)/r)*sum(Tstats);
output=JK;
```

Using the same set of parameters shown in (2.65), I estimated $E(JK(\widehat{P_{rev}}))$ with extensive simulation studies as before. These estimates and their relative bias are given below, and can be compared with tables (2.67) and (2.68).

$\mathbf{s = m = 25}$	$\sigma_d = 4$	$\sigma_d = 6$	$\sigma_d = 8$
$\sigma_D = 40$	$2,1550 \times 10^{-4}$	$2,2565 \times 10^{-4}$	$2,4030 \times 10^{-4}$
	$(0,0244)$	$(0,0294)$	$(0,0357)$
$\sigma_D = 50$	$2,6116 \times 10^{-3}$	$2,6550 \times 10^{-3}$	$2,7165 \times 10^{-3}$
	$(0,1010)$	$(0,0999)$	$(0,0984)$
$\sigma_D = 60$	$9,8693 \times 10^{-3}$	$9,9513 \times 10^{-3}$	$1,0067 \times 10^{-2}$
	$(0,0639)$	$(0,0634)$	$(0,0627)$

(2.76)

and

$\mathbf{s = m = 50}$	$\sigma_d = 4$	$\sigma_d = 6$	$\sigma_d = 8$
$\sigma_D = 40$	$2,0955 \times 10^{-4}$	$2,1871 \times 10^{-4}$	$2,3196 \times 10^{-4}$
	$(-0,0039)$	$(-0,0023)$	$(-0,0003)$
$\sigma_D = 50$	$2,4216 \times 10^{-3}$	$2,4637 \times 10^{-3}$	$2,5232 \times 10^{-3}$
	$(0,0209)$	$(0,0206)$	$(0,0202)$
$\sigma_D = 60$	$9,3813 \times 10^{-3}$	$9,4627 \times 10^{-3}$	$9,5770 \times 10^{-3}$
	$(0,0113)$	$(0,0112)$	$(0,0110)$

(2.77)

It is clear that the jackknife estimator reduces the bias of $\widehat{P_{rev}}$ significantly.

2.9. Obtaining a confidence interval for P_{rev}

The jackknife estimators $JK(\widehat{P_{rev}})$ and $JK(\widehat{P(R)})$ might be very good point estimators of P_{rev} and $P(R)$, but it will be helpful to have some indication of range as well. In this section I shall look at a method of developing confidence intervals for P_{rev} and $P(R)$.

Consider

$$\hat{\lambda} = \frac{-\hat{\mu}}{\sqrt{S_d^2 + 2S_D^2}} = f(\hat{\mu}_d, \hat{\sigma}_d^2, \hat{\sigma}_D^2) \tag{2.78}$$

with the individual estimators defined as in (2.59).

The first order Taylor series expansion around the true parameter value $(\mu_d, \sigma_d^2, \sigma_D^2)$ is

$$\begin{aligned}
\hat{\lambda} &\approx f(\mu_d, \sigma_d^2, \sigma_D^2) + (\hat{\mu}_d - \mu_d)\tfrac{\partial f}{\partial \mu_d}(\mu_d, \sigma_d^2, \sigma_D^2) \\
&\quad +(\hat{\sigma}_d^2 - \sigma_d^2)\tfrac{\partial f}{\partial \sigma_d^2}(\mu_d, \sigma_d^2, \sigma_D^2) + (\hat{\sigma}_D^2 - \sigma_D^2)\tfrac{\partial f}{\partial \sigma_D^2}(\mu_d, \sigma_d^2, \sigma_D^2) \\
&= \lambda + (\hat{\mu}_d - \mu_d)\tfrac{\partial f}{\partial \mu_d}(\mu_d, \sigma_d^2, \sigma_D^2) \\
&\quad +(\hat{\sigma}_d^2 - \sigma_d^2)\tfrac{\partial f}{\partial \sigma_d^2}(\mu_d, \sigma_d^2, \sigma_D^2) + (\hat{\sigma}_D^2 - \sigma_D^2)\tfrac{\partial f}{\partial \sigma_D^2}(\mu_d, \sigma_d^2, \sigma_D^2).
\end{aligned} \tag{2.79}$$

Now,

$$\begin{aligned}\frac{\partial f}{\partial \mu_d}(\mu_d, \sigma_d^2, \sigma_D^2) &= \frac{\partial}{\partial \mu_d}\left(\frac{-\mu_d}{\sqrt{\sigma_d^2+2\sigma_D^2}}\right) \\ &= \frac{-1}{\sqrt{\sigma_d^2+2\sigma_D^2}} \cdot \frac{\mu_d}{\mu_d} \\ &= \frac{\lambda}{\mu_d}.\end{aligned} \tag{2.80}$$

$$\begin{aligned}\frac{\partial f}{\partial \sigma_d^2}(\mu_d, \sigma_d^2, \sigma_D^2) &= \frac{\partial}{\partial \sigma_d^2}\left(\frac{-\mu_d}{\sqrt{\sigma_d^2+2\sigma_D^2}}\right) \\ &= \frac{\mu_d}{2\left(\sigma_d^2+2\sigma_D^2\right)^{3/2}} \cdot \frac{\mu_d^2}{\mu_d^2} \\ &= \frac{-\lambda^3}{2\mu_d^2}.\end{aligned} \tag{2.81}$$

$$\begin{aligned}\frac{\partial f}{\partial \sigma_D^2}(\mu_d, \sigma_d^2, \sigma_D^2) &= \frac{\partial}{\partial \sigma_D^2}\left(\frac{-\mu_d}{\sqrt{\sigma_d^2+2\sigma_D^2}}\right) \\ &= \frac{\mu_d}{\left(\sigma_d^2+2\sigma_D^2\right)^{3/2}} \cdot \frac{\mu_d^2}{\mu_d^2} \\ &= \frac{-\lambda^3}{\mu_d^2}.\end{aligned} \tag{2.82}$$

Substituting (2.80), (2.81) and (2.82) into (2.79), we have that

$$\hat{\lambda} \approx \lambda + (\hat{\mu}_d - \mu_d)\frac{\lambda}{\mu_d} + (\hat{\sigma}_d^2 - \sigma_d^2)\left(\frac{-\lambda^3}{2\mu_d^2}\right) + (\hat{\sigma}_D^2 - \sigma_D^2)\left(\frac{-\lambda^3}{\mu_d^2}\right). \tag{2.83}$$

Note that

$$\begin{aligned}\hat{\mu}_d - \mu_d &= \bar{x}_d - \mu_d &=_{\mathcal{L}}\quad & N(0, \tfrac{\sigma_d^2}{m}) \\ \hat{\sigma}_d^2 - \sigma_d^2 &= S_d^2 - \sigma_d^2 &\approx_{\mathcal{L}}\quad & N(0, \tfrac{2\left(\sigma_d^2\right)^2}{s-1}) \\ \hat{\sigma}_D^2 - \sigma_D^2 &= S_D^2 - \sigma_D^2 &\approx_{\mathcal{L}}\quad & N(0, \tfrac{2\left(\sigma_D^2\right)^2}{m-1}).\end{aligned} \tag{2.84}$$

Therefore, using (2.83) and (2.84),

$$\hat{\lambda} \approx_{\mathcal{L}} N(\lambda, g(\lambda, \mu_d, \sigma_d^2, \sigma_D^2, s, m)) \tag{2.85}$$

where, making the realistic assumption that $\sigma_d/\mu_d \approx 0$,

$$\begin{aligned} & g(\lambda, \mu_d, \sigma_d^2, \sigma_D^2, s, m) \\ = & \left(\frac{\lambda}{\mu_d}\right)^2 \cdot \frac{\sigma_d^2}{m} + \left(\frac{-\lambda^3}{2\mu_d^2}\right)^2 \cdot \frac{2\left(\sigma_d^2\right)^2}{s-1} + \left(\frac{-\lambda^3}{\mu_d^2}\right)^2 \cdot \frac{2\left(\sigma_D^2\right)^2}{m-1} \\ = & \frac{\lambda^2\sigma_d^2}{\mu_d^2 m} + \frac{\lambda^6 2\sigma_d^4}{4\mu_d^4(s-1)} + \frac{\lambda^6 2\sigma_D^4}{\mu_d^4(m-1)} \\ \approx & \frac{\lambda^6 2\sigma_D^4}{\mu_d^4(m-1)} \\ \approx & \frac{\lambda^6}{2(m-1)} \cdot \frac{1}{\lambda^4} \\ = & \frac{\lambda^2}{2(m-1)}. \end{aligned} \tag{2.86}$$

Note that the approximated variance of $\hat{\lambda}$ is a quadratic function of the mean. This enables us to derive a confidence interval for P_{rev} using a log-transformation. We shall need the following theorem.

Theorem 2.1. *Let* $\{T_n\}, n = 1, 2, 3, \ldots$ *be a sequence of statistics such that*

$$\sqrt{n}(T_n - \theta) \xrightarrow{\mathcal{L}} X =_{\mathcal{L}} N(0, \sigma^2(\theta)). \tag{2.87}$$

Let g *be a function of a single variable admitting the first derivative* g' *in the*

point θ. Then

$$\sqrt{n}\,(g(T_n) - g(\theta)) \xrightarrow{\mathcal{L}} X =_{\mathcal{L}} N(0, \left[g'(\theta)\sigma(\theta)\right]^2). \tag{2.88}$$

(see Rao (1965) p.319 for a proof).

In our case, we can define

$$\begin{aligned} T_n &= \hat{\lambda} \\ g(\lambda) &= \log(-\lambda) \\ \sigma^2(\lambda) &= \tfrac{\lambda^2}{2(m-1)} \end{aligned} \tag{2.89}$$

and from (2.88)

$$\begin{aligned} \log(-\hat{\lambda}) &\approx_{\mathcal{L}} N(\log(-\lambda), \tfrac{\lambda^2}{2(m-1)} \cdot \left(\tfrac{-1}{\lambda}\right)^2) \\ &= N(\log(-\lambda), \tfrac{1}{2(m-1)}). \end{aligned} \tag{2.90}$$

or alternatively

$$\sqrt{2(m-1)}(\log(-\hat{\lambda}) - \log(-\lambda)) \approx_{\mathcal{L}} N(0,1). \tag{2.91}$$

This enables us to derive an approximate $(1-\alpha)$ confidence interval for P_{rev}.

$$\begin{aligned} 1-\alpha &= P(-Z_{\alpha/2} \leq \sqrt{2(m-1)}(\log(-\hat{\lambda}) - \log(-\lambda)) \leq Z_{\alpha/2}) \\ &= P(\hat{\lambda}\exp\left(\frac{Z_{\alpha/2}}{\sqrt{2(m-1)}}\right) \leq \lambda \leq \hat{\lambda}\exp\left(\frac{-Z_{\alpha/2}}{\sqrt{2(m-1)}}\right)). \end{aligned} \tag{2.92}$$

A $(1-\alpha)$ confidence interval for λ is therefore

$$\left[\hat{\lambda}\exp\left(\frac{Z_{\alpha/2}}{\sqrt{2(m-1)}}\right); \hat{\lambda}\exp\left(\frac{-Z_{\alpha/2}}{\sqrt{2(m-1)}}\right)\right] \tag{2.93}$$

and hence

$$\left[\Phi\left(\hat{\lambda}\exp\left(\frac{Z_{\alpha/2}}{\sqrt{2(m-1)}}\right)\right); \Phi\left(\hat{\lambda}\exp\left(\frac{-Z_{\alpha/2}}{\sqrt{2(m-1)}}\right)\right)\right] \tag{2.94}$$

is a $(1-\alpha)$ confidence interval for P_{rev}. See Chapter 6 for examples of the use of (2.94).

3. The Initiation Front

3.1. Definition

Apart from the reversal probability discussed in Chapter 2, the other basic parameter that is of extreme importance in sequential blasting processes is the *initiation front.* Most generally we can define a sequence of initiation fronts $I_1, I_2, \ldots$ where I_r equals the number of main delays ahead of the rth that have been initiated at the instant when the rth explodes, i.e.

$$I_r = \begin{cases} \max\limits_{j \in \mathbb{N}} \{d_r + d_{r+1} + \ldots + d_{r+j-1} \leq D_r\} & \text{if } d_r \leq D_r \\ 0 & \text{if } d_r > D_r. \end{cases} \tag{3.1}$$

Note that

- (3.1) applies only to the standard sequential setup, as depicted in figure (2.2). The definitions for other patterns are similar, but I shall restrict my focus to the standard setup.
- for all practical purposes, $d_r < D_r$ almost surely, but the event is nonetheless accounted for in definition (3.1).
- I_r is defined on a conceptually infinite sequential array of main and surface delays. Once the final main delay in a finite sequence has been ignited, the concept of an initiation front is meaningless.

- I_r is a discrete random variable taking on non-negative integer values, but is a function of the independent continuous random variables $d_r, \ldots, d_{r+j-1}$ and D_{r+1}.

- I_r and I_{r+s} are identically distributed, but not independent. In fact, they are highly correlated for small s.

- A special case is

$$I := I_1 = \max_{j \in \aleph} \{d_1 + d_2 + \ldots + d_j \leq D_1\}, \tag{3.2}$$

the number of main delays (excluding the first) already initiated when the first explosion in the sequence occurs.

The remainder of this chapter will focus only on the special case I, as all the results can be easily generalised to apply to I_r.

3.2. The Distribution of I

From (3.2)

$$\begin{aligned} P(I \geq b) &= P(D_1 \geq d_1 + \ldots + d_b) \\ &= P(D_1 - d_1 - \ldots - d_b \geq 0) \\ &= \Phi\left(\frac{\mu_D - b \cdot \mu_d}{\sqrt{\sigma_D^2 + b \cdot \sigma_d^2}}\right). \end{aligned} \tag{3.3}$$

Therefore the probability mass function of I is

$$\begin{aligned} f_I(b) &= P(I \geq b) - P(I \geq b+1) \\ &= \begin{cases} \Phi\left(\frac{\mu_D - b\cdot\mu_d}{\sqrt{\sigma_D^2 + b\cdot\sigma_d^2}}\right) - \Phi\left(\frac{\mu_D - (b+1)\cdot\mu_d}{\sqrt{\sigma_D^2 + (b+1)\cdot\sigma_d^2}}\right) & b \in \aleph \\ 0 & \text{otherwise.} \end{cases} \end{aligned} \tag{3.4}$$

The mass function f_I can be re-parameterised in terms of $k = \frac{\mu_D}{\mu_d}$, the ratio of the main delay mean to that of the surface delay mean. For $b \in \aleph$,

$$f_I(b) = \Phi\left(\frac{\mu_d(k-b)}{\sqrt{\sigma_D^2 + b\cdot\sigma_d^2}}\right) - \Phi\left(\frac{\mu_d(k-b-1)}{\sqrt{\sigma_D^2 + (b+1)\cdot\sigma_d^2}}\right). \tag{3.5}$$

Note that (3.4) and (3.5) can easily be calculated in any specific instance. The following Matlab m-function illustrates how this can be implemented on a numerical package.

```
function output = ifront(mu_surf,mu_main,s_surf,s_main)
middle=fix(mu_main/mu_surf);
for i=(middle-4):(middle+4);
arg1=(mu_main-i*mu_surf)/sqrt(s_main^2+i*s_surf^2);
arg2=(mu_main-(i+1)*mu_surf)/sqrt(s_main^2+(i+1)*s_surf^2);
distr(i-middle+5,1)=i;
distr(i-middle+5,2)=normcdf(arg1)-normcdf(arg2);
end;
output=distr;
```

The cases where $k \in \aleph$ and $(k - \frac{1}{2}) \in \aleph$ are of particular theoretical interest, as the following example will illustrate.

Example 2. *Consider the following two cases.*

	Case 1	*Case 2*
k	$20,0$	$20,5$
μ_d	200	200
σ_D	40	40
σ_d	4	4

(3.6)

The two distributions are depicted in figures (3.1) and (3.2). In the case where k is an integer 20, the distribution is a two-point distribution with the probability mass split evenly between the two points 19 and 20. When k is exactly midway between 20 and 21, most of the mass looks to be concentrated at the point 20, while small amounts can be seen at 19 and 21.

3.3. Expected value

For a given set of parameters, the moments of I can be calculated to any desired degree of numerical accuracy. However, general insight into the behaviour of I can be obtained by developing a heuristic approximation to $E(I)$.

First of all, consider a hypothetical case where the burning times of the main

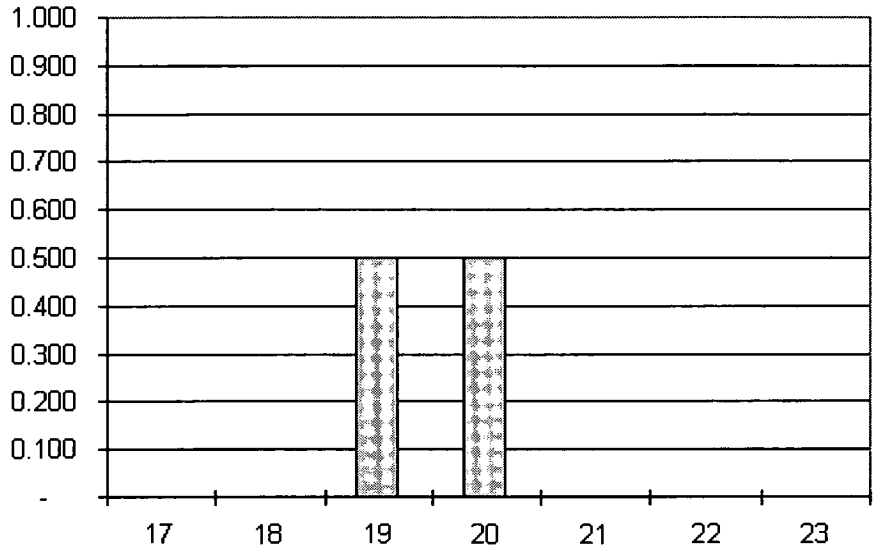

Figure 3.1: Distribution of I, $k = 20,0$

and surface delays are not subject to statistical variation, i.e. D_i and d_i are constants. In this case, the burning front will also be a constant. Substituting μ_D and μ_d for D_1 and d_i in (3.2) yields

$$I = \max_{j \in \mathbb{N}} \left\{ j \leq \frac{\mu_D}{\mu_d} \right\} = \left\lfloor \frac{\mu_D}{\mu_d} \right\rfloor . \tag{3.7}$$

For example, if the main delay D_1 is always 4 500 ms and the surface delays always 200 ms, then $I = \left\lfloor \frac{4\,500}{200} \right\rfloor = 22$.

In reality, of course, burning times are subject to statistical variation. As a

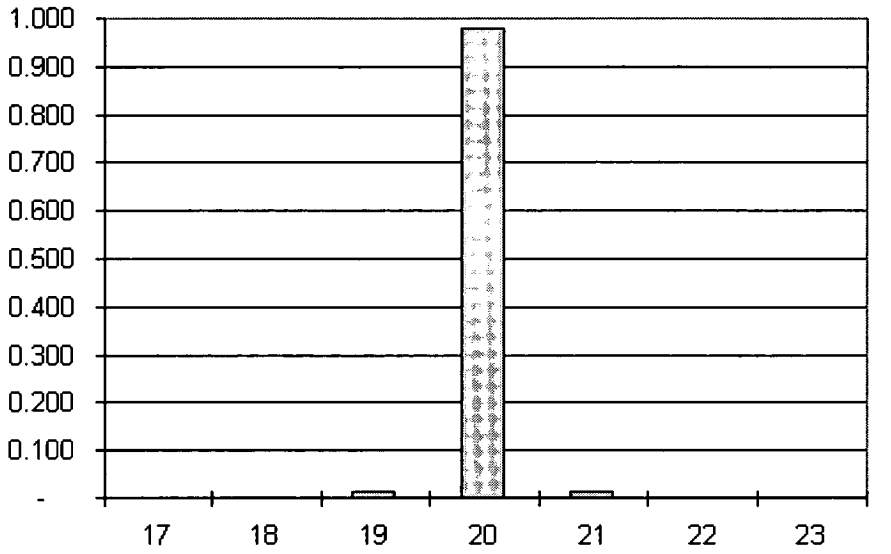

Figure 3.2: Distribution of I, $k = 20, 5$

first step, we could develop some bounds for $E(I)$. From definition (3.2),

$$d_1 + \ldots + d_I \leq D_1. \tag{3.8}$$

It is easy to see that I is a stopping time, since the event $\{I = k\}$ is a function of $d_1, \ldots d_k$ and the state of the first main delay at time $(d_1 + \ldots + d_k)$ only. This allows us to make use of Wald's equation (see Grimmett and Stirzaker (1992) for a proof).

Lemma 1 (Wald's equation). *Let $X_1, X_2, \ldots$ be independent identically distributed random variables with finite mean, and let M be a stopping time with*

respect to the X_i satisfying $E(M) < \infty$. Then

$$E\left(\sum_{i=1}^{M} X_i\right) = E(X_i)E(M). \tag{3.9}$$

Applying (3.9) to (3.8),

$$\begin{aligned} & E(I)E(d_i) \leq E(D_1) \\ \Rightarrow \quad & E(I) \leq \tfrac{\mu_D}{\mu_d}. \end{aligned} \tag{3.10}$$

Also from definition (3.2),

$$d_1 + \ldots + d_{I+1} > D_1. \tag{3.11}$$

$I+1$ is also a stopping time, since the event $\{I+1=k\} \Rightarrow \{I=k-1\}$ is a function of $d_1, \ldots d_{k-1}$ and the state of the first main delay at time $(d_1 + \ldots + d_{k-1})$ only. Therefore

$$\begin{aligned} & E(I+1)E(d_i) > E(D_1) \\ \Rightarrow \quad & E(I) > \tfrac{\mu_D}{\mu_d} - 1. \end{aligned} \tag{3.12}$$

Hence, by (3.10) and (3.12),

$$-1 < E(I) - \frac{\mu_D}{\mu_d} \leq 0. \tag{3.13}$$

As a first thought one might be tempted to use $\frac{\mu_D}{\mu_d}$ as an estimate of $E(I)$. This is incorrect, though, because the initiation front is a sum of continuous random variables that is reduced by $\frac{1}{2}$ on average, due to the rounding down effect of truncation. A much better estimate of $E(I)$ is

$$\widehat{E(I)} = \frac{\mu_D}{\mu_d} - \frac{1}{2}. \tag{3.14}$$

3.3.1. The special case $k \in \aleph$

Suppose that k is an integer, i.e. the mean of the main delays is some integer multiple of the mean of the surface delays, and that σ_d is relatively small compared to μ_d (as is the case in practice). Then

$$\begin{aligned} f_I(k) &= \Phi\left(\frac{\mu_d(k-k)}{\sqrt{\sigma_D^2+k\cdot\sigma_d^2}}\right) - \Phi\left(\frac{\mu_d(k-k-1)}{\sqrt{\sigma_D^2+(k+1)\cdot\sigma_d^2}}\right) \\ &= \Phi(0) - \Phi\left(\frac{-\mu_d}{\sqrt{\sigma_D^2+(k+1)\cdot\sigma_d^2}}\right) \\ &\approx 0,5 - P_{rev} \\ &\approx 0,5 \end{aligned} \tag{3.15}$$

Furthermore,

$$\begin{aligned} f_I(k-1) &= \Phi\left(\frac{\mu_d(k-k+1)}{\sqrt{\sigma_D^2+(k-1)\cdot\sigma_d^2}}\right) - \Phi\left(\frac{\mu_d(k-k+1-1)}{\sqrt{\sigma_D^2+k\cdot\sigma_d^2}}\right) \\ &= \Phi\left(\frac{\mu_d}{\sqrt{\sigma_D^2+(k-1)\cdot\sigma_d^2}}\right) - \Phi(0) \\ &\approx (1-P_{rev}) - 0,5 \\ &\approx 0,5 - P_{rev} \\ &\approx 0,5. \end{aligned} \tag{3.16}$$

Therefore, when the expected burning time of the main delays is an integer multiple k of the expected burning times of the surface delays, the initiation front will most likely be either k or $k-1$, both with approximately equal probability of $0,5$. However, note that

$$\frac{\mu_d}{\sqrt{\sigma_D^2+(k+1)\cdot\sigma_d^2}} < \frac{\mu_d}{\sqrt{\sigma_D^2+(k-1)\cdot\sigma_d^2}} \tag{3.17}$$

so that, from (3.15) and (3.16),

$$f_I(k) < f_I(k-1) < 0,5. \tag{3.18}$$

A small amount of probability mass, $1-(f_I(k-1)+f_I(k))$, is therefore distributed in the points to the right of k and to the left of $k-1$. This is illustrated by the

following distribution with unrealistically large σ_d and σ_D:

$$\mu_d = 200 \qquad \sigma_d = 8$$

$$\mu_D = 3\,800 \qquad \sigma_D = 80$$

x	$f_I(x)$
15	$1,6587 \times 10^{-12}$
16	$1,8957 \times 10^{-6}$
17	$1,0682 \times 10^{-2}$
18	$4,8932 \times 10^{-1}$
19	$4,8876 \times 10^{-1}$
20	$1,1237 \times 10^{-2}$
21	$2,7408 \times 10^{-6}$
22	$5,5996 \times 10^{-12}$

(3.19)

3.3.2. The special case $(k - \frac{1}{2}) \in \aleph$

Consider the case $k - \frac{1}{2} = i \in \aleph$. Then

$$\begin{aligned} f_I(i) &= \Phi\left(\frac{\mu_D - i\cdot\mu_d}{\sqrt{\sigma_D^2 + i\cdot\sigma_d^2}}\right) - \Phi\left(\frac{\mu_D - (i+1)\cdot\mu_d}{\sqrt{\sigma_D^2 + (i+1)\cdot\sigma_d^2}}\right) \\ &= \Phi\left(\frac{\mu_d}{2\sqrt{\sigma_D^2 + k\cdot\sigma_d^2 - \sigma_d^2/2}}\right) - \Phi\left(\frac{-\mu_d}{2\sqrt{\sigma_D^2 + k\cdot\sigma_d^2 + \sigma_d^2/2}}\right) \\ &\approx 1 - 2\cdot\Phi\left(\frac{-\mu_d}{2\sqrt{\sigma_D^2 + k\cdot\sigma_d^2 + \sigma_d^2/2}}\right) \\ &\approx 1 - 2P_{rev}. \end{aligned} \tag{3.20}$$

Most of the distribution's mass will be concentrated at the point $k-\frac{1}{2}$, with the remainder being split among the points in the vicinity of $k-\frac{1}{2}$. This is illustrated by the following distribution:

$$\mu_d = 200 \qquad \sigma_d = 8$$

$$\mu_D = 3\,900 \qquad \sigma_D = 80$$

x	$f_I(x)$
15	2.2204×10^{-16}
16	3.7768×10^{-9}
17	2.7806×10^{-4}
18	1.2565×10^{-1}
19	7.4716×10^{-1}
20	1.2659×10^{-1}
21	3.2589×10^{-4}
22	7.6358×10^{-9}
23	1.5543×10^{-15}

(3.21)

3.3.3. $E(I)$ and $var(I)$ in relation to k

Figure (3.3) depicts $E(I)$ against k for $k \in [19;20]$, as well as $\widehat{E(I)} = k - \frac{1}{2}$ and the upper and lower bounds for $E(I)$ developed in (3.13).

The estimator $k - \frac{1}{2}$ seems to be a reasonably good linear estimator of $E(I)$,

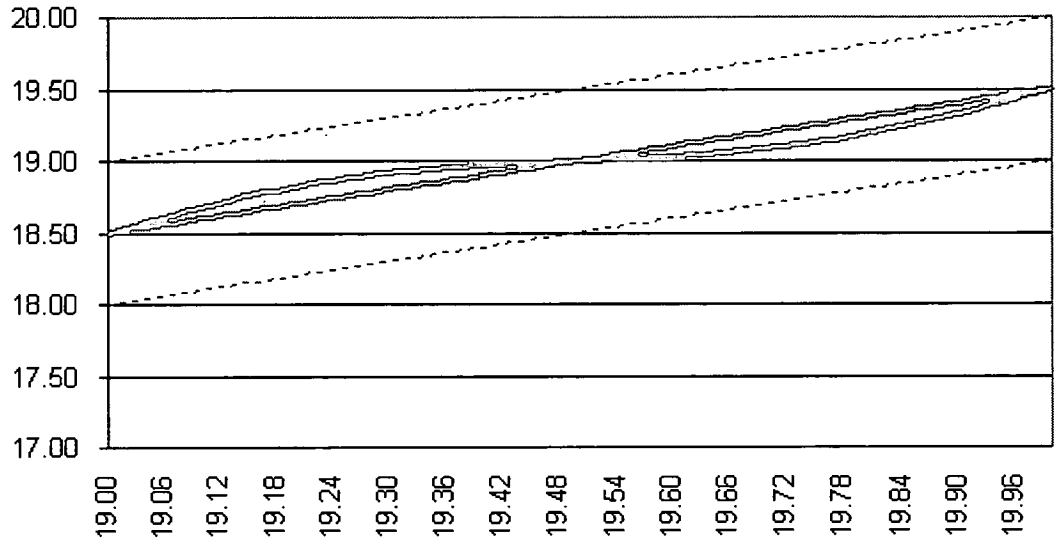

Figure 3.3: $E(I)$ in black, $k-\frac{1}{2}$ in light grey, and bounds for $E(I)$, for $19 \leq k \leq 20$.

especially in the two special cases $k \in \aleph$ and $k - \frac{1}{2} \in \aleph$, as is often the case in practice.

Figure (3.4) depicts $var(I)$ against k for $k \in [19; 20]$. It is clear that $var(I)$ is maximised when $k \in \aleph$ and minimised when $k - \frac{1}{2} \in \aleph$.

3.4. I versus $P(R)$

From a practical point of view, the burning front of a sequential array of detonators should be as large as possible. This ensures that dislodged material from explosions do not cut trunk lines that are still to initiate detonators to come. Increasing the initiation front means increasing μ_D in relation to μ_d. However,

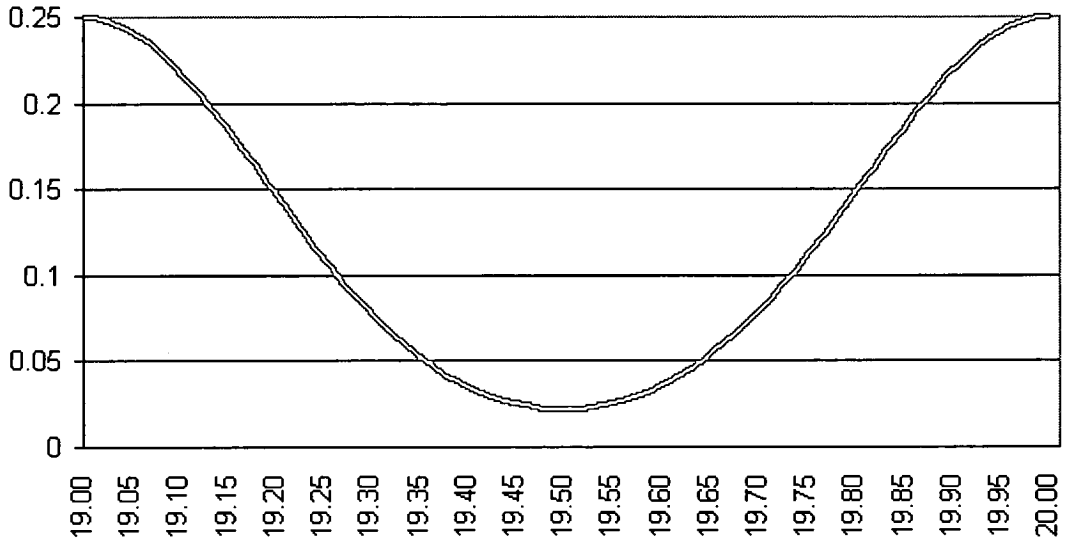

Figure 3.4: $var(I)$ against k

there is strong empirical evidence (obtained from industry quality control samples) suggesting that σ_D increases, at least linearly, with μ_D. This increase in σ_D necessarily leads to an increase in $P(R)$, the probability of a failed blasting sequence.

Conversely, to decrease the reversal probability, one needs to decrease σ_D. This can only be accomplished by reducing μ_D, which results in a shortened burning front. This is the trade-off between the initiation front and the reversal probability that was referred to in Chapter 1. From a quality control point of view, it is clear that controlling μ_D only controls the initiation front. To control $P(R)$, one also needs to control σ_D.

4. Testing for Normality

4.1. Introduction

In the previous chapters it was assumed that the burning times of the main and surface delays were independently identically normally distributed with means μ_D and μ_d and variances σ_D^2 and σ_d^2 respectively. While this allowed explicit calculation of quantities such as the probability of pairwise reversal and the distribution of the initiation front, such normality assumptions need not hold in practice.

The purpose of this chapter is to develop on-line methods of checking whether the normality assumptions are indeed reasonable.

4.2. Survey of existing literature

Suppose that $X_1, X_2, \ldots, X_n$ are n statistically independent random variables with the same (unknown) distribution function, $F_X(x) = P(X \leq x)$, and it is required to test the hypothesis that F_X is some theoretical distribution function. Particular attention has been paid to testing whether the X_i are normally distributed with common (unknown) parameters μ and σ^2. One of the most widely used tests of normality is Pearson's χ^2-test. For a complete discussion, see Chernoff and Lehmann (1954) or Mann and Wald (1942). Anderson and Darling (1952 and 1954) developed some tests of normality goodness-of-fit based on a variety of chi-squared type "distance" methods. Kac, Kiefer and Wolfowitz (1955) extended

their work by considering the asymptotic power of these tests.

The Kolmogorov-Smirnov test is also widely used for testing normality when the mean and variance of the X_i are known; see Massey (1951). Lilliefors (1967) showed how the Kolmogorov-Smirnov test can be modified to take estimation of the unknown parameters into account and he found some critical values of the test statistic by means of simulation.

The above tests all refer to a single sample of i.i.d. observations. However, suppose we have available k independent samples, with the jth sample of size n_j, i.e.

$$\begin{array}{lllll} \tilde{x}_1 = & x_{11}, & x_{12}, & \ldots & x_{1n_1} \\ \tilde{x}_2 = & x_{21}, & x_{22}, & \ldots & x_{2n_2} \\ \vdots & \vdots & \vdots & \ddots & \vdots \\ \tilde{x}_k = & x_{k1}, & x_{k2}, & \ldots & x_{kn_k} \end{array} \tag{4.1}$$

Suppose further that one is interested in testing the hypothesis that **all k of the samples in (4.1) are normally distributed**, possibly all with different parameters. (4.1) is said to *adhere to a normal model* if the j th sample is distributed $N(\mu_j, \sigma_j^2)$ for all $j = 1 \ldots k$. It is thus required to construct a k-sample composite goodness-of-fit test.

Unlike the voluminous literature on single-sample normality testing, there is very little published material available on composite sample fitting techniques.

Petrov (1956) did some theoretical work on models of type (4.1) and stated some distributional results when all the samples are of a common size $n_j = n$. Prohorov (1966) suggested a transformation-pooling approach which was eventually fully developed by Quesenberry et al (1976).

The relative lack of interest in multiple sample normality testing might be due to the fact that, in most practical situations, "small" deviations from normality are often not thought to be critical. However, the properties of the results concerning the sequential blasting processes developed in this dissertation all require that normality holds, especially in the tail areas of the distributions.

4.3. Quesenberry's transformation-pooling technique

For the j th sample in (4.1), Quesenberry et al defined $(n_j - 2)$ so-called u-statistics as follows:

$$u_{j,(r-2)} := T_{r-2}\left\{\frac{\sqrt{r-2}\cdot(x_{jr}-\bar{x}_{jr})}{\sqrt{(r-1)s_{jr}^2-(x_{jr}-\bar{x}_{jr})^2}}\right\} \qquad j=1\ldots k;\ r=3\ldots n_j \quad (4.2)$$

The $(n_j - 2)$ u-statistics of the jth sample will be independently and identically distributed $U[0;1]$ random variables, **if** the jth sample is indeed from a $N(\mu_j, \sigma_j^2)$ distribution. All the u-statistics are then pooled together and sorted, to end up with $N = (n_1 + \ldots + n_k - 2k)$ values. Under the normal model hypothesis, $E(u_{(j)}) = \frac{j}{N+1}$. The pairs $(u_{(j)}; \frac{j}{N+1})$ are then plotted on the usual xy plane and

the points should approximate the line $y = x$. This provides a graphical method of judging whether the normal hypothesis should be rejected or not.

The original problem of testing for normality of multiple samples is thus reduced to determining whether the N derived u-transformations are from a $U[0, 1]$ distribution, the more common goodness-of-fit hypothesis testing problem.

4.4. Disadvantages of pooling

Although the procedure described above provides an intuitive basis for multiple sample normality testing, it does have a few inherent disadvantages:

- If the uniformity hypothesis (and thus the original normality hypothesis) is rejected, the procedure does not give any indication which of the k samples deviate from normality. It could very well be that only one sample differs substantially from the normal distribution. A better procedure would also indicate "trouble spots" while it is being applied.

- The suggested u-transformation loses two observations for each sample. The original dataset is thus reduced by $2k$ values. This could potentially be disruptive, especially when working with a large number of relatively small samples.

- The major disadvantage, however, is that the transformations described in (4.2) are not symmetric in the observations. This means that a different set

of u-values will be obtained if the observations in each sample are numbered differently, a rather unsatisfactory characteristic of the procedure. Quesenberry suggested a randomisation of the sample, which would mean that two different analysts, using the same procedure on the same data set, would arrive at two different test statistics and, hence, different decisions.

4.5. The Anderson-Darling Statistic

Returning for the moment to the problem of testing for normality in the single sample case, consider a sample of size n from some unknown distribution. If the sample is denoted by $X_1, \ldots, X_n$, then the standardised variables will be denoted by $Z_1, \ldots, Z_n$, where

$$Z_i := \frac{X_i - \bar{X}}{S_X}. \tag{4.3}$$

The empirical distribution function of the Z_i is

$$F_n(x) = \frac{1}{n} \sum_{i=1}^{n} ind(Z_i \leq x) \tag{4.4}$$

and the Anderson-Darling statistic is

$$A_n^2 := n \cdot \int_{-\infty}^{\infty} \frac{(F_n(x) - \Phi(x))^2}{x(1-x)} dx. \tag{4.5}$$

A practical formula for calculating A_n^2 is given by Shorack and Wellner (1986,

p.227) as

$$A_n^2 = \frac{1}{n}\sum_{j=1}^{n}(2j-1)\log\frac{1}{\xi_{(i)}(1-\xi_{(n-j+1)})} \tag{4.6}$$

where $\xi_{(i)}$ is the ith order statistic of $\{\xi_i := \Phi(Z_i)\}$. The following Matlab m-function will calculate (4.6):

```
function a=a2n(X)
[n,p]=size(X);
if n==1;X=X';n=p;end;
stdizedx=((X-ones(n,1)*mean(X))./(ones(n,1)*std(X)));
xi=sort(normcdf(stdizedx));
weights=1:2:(2*n-1);
a=(weights*(-log(xi))-weights*log(1-flipud(xi)))/n-n;
```


We are now able to devise a type of control chart, based on the Anderson-Darling statistic, that will allow for continuous normality testing in a manufacturing process.

4.6. The Control Chart Approach

The control chart is a popular on-line method for evaluating and monitoring a certain statistical characteristic of a production process. The general theory of control charts was first proposed and developed by Dr. Walter A. Shewhart, and any control chart developed according to these principles is commonly referred to as a Shewhart-type control chart, or just a Shewhart chart.

In a production process such as that used for the manufacturing of detonators, there will always exist a certain level of natural variability or "background noise", which comprises of many small, mostly unavoidable causes. Most manufacturers and quality controllers will consider a "relatively small" level of background noise to be perfectly acceptable, as it is the necessary result of living in an imperfect world. This natural variability is often called a "stable system of chance causes", or more modernly, a "stable system of common causes". A certain characteristic of a production system (such as its mean) is said to be *in statistical control* if only common causes of variation are present in that characteristic.

There are essentially three major sources of "unnatural" variability in a production process, namely

- improperly adjusted machines,
- operator errors, and
- defective raw materials.

Variability arising from one or more of the above sources (referred to as "assignable" or "special" causes) is usually orders of magnitude larger than normal background noise and most manufacturers would consider such variability to be unacceptable. Such a process is said to be *out of control.*

The main objective of an on-line statistical control procedure is to quickly

detect the presence of an assignable cause of variability or a shift in the characteristics of the process being monitored. As will be seen later, however, the rapid response of such a system must be balanced against too many false alarms which interrupt the production process too frequently. As is the case with most choices in life, a compromise needs to be found.

A control chart is usually implemented in a graphic way, plotting a certain statistic over time as the sampled values are fed into the system. This by itself is already an indicator of how the process behaves over time, but one still needs a method of quantifying exactly when the process is "out of control". In the traditional Shewhart-type chart, three horizontal lines are also plotted on the graph, namely

- a **Centre Line**, representing the statistical mean of the characteristic being monitored,
- the **Upper Control Limit,** and
- the **Lower Control Limit**,

the latter two being chosen so that nearly all of the plotted values should fall between these two lines if the process is in control. Quantifying what is meant by "nearly all values" constitutes the major part of developing a control chart.

4.7. Strategy for monitoring normality

The statistic that I shall use as an indicator for deviation from normality, especially in the tail areas, is A_n^2, the Anderson-Darling statistic. In this case, consistently large observed values of A_n^2 indicate deviation from normality, while smaller values indicate that the process is in control, i.e. that the underlying process is approximately normally distributed. Since normality is in question only when A_n^2 has a large value, any control chart based on this statistic will have only an upper control limit. It is thus necessary to find the upper percentiles for the statistic, and since it depends on the sample size n, this needs to be calculated for a range of values. The limiting distribution's percentiles will be approximated by choosing n to be "sufficiently large".

4.8. Finding upper percentiles for A_n^2

To find the approximate percentage points for A_n^2, I used extensive simulation studies. The general procedure is as follows:

- Generate (say) 20 000 sets of n sample values from a $N(0,1)$ distribution.
- Calculate A_n^2 for each of these 20 000 sample sets.
- Sort the vector of A_n^2 statistics.

- Approximate the 90th through 99,5th percentiles by recording the vector values with indices corresponding to the relevant percentiles.

I repeated this procedure for $n = 10, 15, 20, 25, 30, 35$ and finally, to approximate the limiting distribution, for $n = 100$. The various percentiles are listed below.

n	10,0%	9,5%	9,0%	8,5%	8,0%	7,5%	7,0%	6,5%	6,0%	5,5%
10	0,584	0,592	0,601	0,609	0,618	0,629	0,640	0,652	0,666	0,678
15	0,593	0,600	0,609	0,619	0,628	0,638	0,650	0,661	0,674	0,688
20	0,606	0,616	0,625	0,635	0,647	0,658	0,668	0,681	0,695	0,709
25	0,609	0,617	0,626	0,636	0,645	0,655	0,668	0,683	0,695	0,710
30	0,615	0,624	0,636	0,645	0,654	0,665	0,677	0,691	0,704	0,720
35	0,618	0,627	0,636	0,645	0,656	0,669	0,681	0,692	0,708	0,722
100	0,624	0,633	0,642	0,650	0,661	0,671	0,681	0,694	0,706	0,721

n	5,0%	4,5%	4,0%	3,5%	3,0%	2,5%	2,0%	1,5%	1,0%	0,5%
10	0,693	0,710	0,729	0,753	0,779	0,807	0,840	0,886	0,949	1,054
15	0,705	0,722	0,747	0,767	0,793	0,820	0,856	0,906	0,969	1,080
20	0,725	0,744	0,766	0,795	0,823	0,851	0,888	0,929	0,994	1,095
25	0,728	0,746	0,767	0,788	0,813	0,836	0,874	0,918	0,980	1,115
30	0,734	0,751	0,774	0,793	0,819	0,851	0,886	0,939	1,012	1,148
35	0,735	0,753	0,771	0,795	0,817	0,845	0,885	0,933	1,013	1,126
100	0,737	0,755	0,775	0,798	0,828	0,864	0,903	0,955	1,033	1,156

(4.7)

4.9. The power of the A_n^2-statistic

To investigate the abilities of A_n^2 to distinguish between samples from a normal distribution and those from a distribution that is almost normal but heavier-tailed, I did some more simulation studies, this time generating observations from

non-normal distributions and calculating A_n^2 for those samples. I looked at two general classes of heavier-tailed distributions, namely

- t_m, Student's t distribution with m degrees of freedom, with density function

$$\begin{aligned} & f(x \mid \nu) \\ = \; & \Gamma(\tfrac{\nu+1}{2}) \left(\Gamma(\tfrac{\nu}{2})\right)^{-1} \cdot (\nu\pi)^{-\frac{1}{2}} \cdot (1+\tfrac{x^2}{2})^{-\frac{\nu+1}{2}} \qquad -\infty < x < \infty, \nu = 1, 2, ... \end{aligned} \tag{4.8}$$

- the family of normal distribution mixtures, with density function

$$\begin{aligned} & f(x \mid \xi, \mu, \sigma_0^2, \sigma_a^2) \\ = \; & \tfrac{1}{\sigma_0}\phi(\tfrac{x-\mu}{\sigma_0}) \cdot (1-\xi) + \tfrac{1}{\sigma_a}\phi(\tfrac{x-\mu}{\sigma_a}) \cdot \xi \qquad -\infty < x < \infty, \; 0 < \xi < 1 \end{aligned} \tag{4.9}$$

4.9.1. The t_m distribution

I chose three different t_m distributions to sample from, namely for $m = 3, 6$ and 10. For the different variations of sample sizes n that I used to approximate the A_n^2 percentiles, I once again simulated 20 000 sets of samples of size n from the relevant t_m distribution. I then calculated the fraction of observed A_n^2 values that exceeded the various theoretical percentiles and used these values as estimates of the power of the test. An excerpt from the results are tabulated below.

n	Distribution	10%	7,5%	5%	2,5%	1%
10	t_{10}	0,12	0,10	0,07	0,04	0,02
	t_6	0,16	0,13	0,10	0,06	0,03
	t_3	0,25	0,22	0,18	0,13	0,09
25	t_{10}	0,16	0,13	0,09	0,06	0,03
	t_6	0,23	0,20	0,16	0,11	0,07
	t_3	0,47	0,44	0,38	0,32	0,26
35	t_{10}	0,19	0,15	0,11	0,07	0,04
	t_6	0,30	0,26	0,21	0,15	0,10
	t_3	0,61	0,57	0,53	0,45	0,38
100	t_{10}	0,25	0,21	0,17	0,11	0,06
	t_6	0,46	0,42	0,37	0,28	0,20
	t_3	0,90	0,88	0,86	0,80	0,74

(4.10)

- Since the t_m-distribution's tail thickness increases as the degrees of freedom m decreases, one would expect the power of the test to increase as m decreases. This is confirmed by the simulation results in table (4.10)

- The power also increases as the sample size n increases from 10 through 100. This is to be expected, as it becomes easier to pick up non-normality within a sample as the sample size increases.

4.9.2. The mixture of normals

In order to interpret any simulation studies of the power of A_n^2 with respect to contaminated normal distributions, it is necessary to understand how the mixture variable ξ influences the normality of the mixture distribution. From (4.9) it is clear that $\xi = 0$ will result in a normal distribution. As ξ is increased, the tail

thickness should also increase due to the contamination, but only to the point where the contaminating distribution starts dominating. The tail thickness will then start decreasing again to that of a normal distribution and when $\xi = 1$, the mixture distribution is once again a pure normal distribution with normal tails. But what value of ξ will maximise the tail thickness, and therefore the mixture distribution's deviation from normality? To determine this, we shall need some quantitative measure of what we mean by "tail thickness". A possible quantity (though probably not the only one) is the **kurtosis**, which I shall define here as

$$\mathcal{K}_4 = \frac{\mu_4}{\mu_2^2} \tag{4.11}$$

where μ_n denotes the nth central moment of the random variable in question (see Ruppert (1987) for a further discussion of the interpretation of kurtosis). To evaluate (4.11), we require expressions for the second and fourth moments of the mixture distribution. This will allow us to maximise $\mathcal{K}_4$ with respect to ξ.

A random variable X, which has density function (4.9), can be represented in the form

$$X = (1 - U) \cdot Y + U \cdot Z \tag{4.12}$$

where

$$\begin{aligned} Y &=_{\mathcal{L}} N(0, \sigma_0^2) \\ Z &=_{\mathcal{L}} N(0, \sigma_a^2) \\ P(U = 1) &= \xi = 1 - P(U = 0) \end{aligned} \tag{4.13}$$

and Y, Z and U are statistically independent. It follows immediately that

$$E(X) = 0. \tag{4.14}$$

Also,

$$\begin{aligned} var(X) &= E(X^2) \\ &= E\{E(X^2 \mid U)\} \\ &= (1 - \xi) \cdot \sigma_0^2 + \xi \cdot \sigma_a^2 \end{aligned} \tag{4.15}$$

and, since μ_4 of a normal variable is $3\sigma^4$,

$$\begin{aligned} \mu_4 &= E(X^4) \\ &= (1 - \xi) \cdot 3\sigma_0^4 + \xi \cdot 3\sigma_a^4. \end{aligned} \tag{4.16}$$

Thus

$$\begin{aligned} \mathcal{K}_4(\sigma_0^2, \sigma_a^2, \xi) &:= \frac{\mu_4}{\mu_2^2} \\ &= \frac{3(1-\xi)\sigma_0^4 + 3\xi\sigma_a^4}{\left\{(1-\xi)\sigma_0^2 + \xi\sigma_a^2\right\}^2} \end{aligned} \tag{4.17}$$

which, when expressed in terms of the ratio $\rho = \sigma_a/\sigma_0$ of the two standard

deviations, is

$$\mathcal{K}_4(\rho^2, \xi) = 3\frac{1+\xi(\rho^4-1)}{\{1+\xi(\rho^2-1)\}^2}. \tag{4.18}$$

Note that $\mathcal{K}_4(\rho^2, 0) = 3$ and $\mathcal{K}_4(\rho^2, 1) = 3$, as expected.

Now

$$\begin{aligned} \log(\mathcal{K}_4) &= \log 3 + \log(1 - \xi + \xi\rho^4) - 2\log(1 - \xi + \xi\rho^2) \\ &:= f(\xi, \rho) \end{aligned} \tag{4.19}$$

and we can differentiate and set equal to 0 to get

$$\frac{\partial f}{\partial \xi} = \frac{-1+\rho^4}{1-\xi+\xi\rho^4} - 2\frac{-1+\rho^2}{1-\xi+\xi\rho^2} = 0, \tag{4.20}$$

which can be solved for ξ to obtain

$$\xi = \frac{1}{1+\rho^2}. \tag{4.21}$$

The second derivative, evaluated at $\xi = (1+\rho^2)^{-1}$ is, after some calculation,

$$\left.\frac{\partial^2 f}{\partial \xi^2}\right]_{\xi=(1+\rho^2)^{-1}} = \frac{-(1-\rho^4)^2}{2\rho^4} \leq 0. \tag{4.22}$$

Hence $\mathcal{K}_4$ is maximised at $\xi = \frac{1}{1+\rho^2}$.

To evaluate the power of A_n^2 when the underlying distribution is a mixture of

two normals, I used various combinations of the two parameters ξ and σ_a, with σ_0 taken to be 50. The standard deviation of the contaminating distribution, σ_a, was varied from two to four times the value of σ_0, i.e.e ρ was taken as 2, 3 and 4 respectively. This means that the kurtosis for the three variations of ρ would have been maximised at $\xi = 0,2,\ 0,1$ and $0,06$ respectively. To investigate whether the power of the test decreases as the kurtosis decreases, I took ξ, the fraction of the contaminating distribution, to be $20\%, 50\%$ and 90% respectively. Using these parameters I once again sampled from the various combinations of distributions and estimated the power of the A_n^2 statistic. An excerpt from the results is tabulated below.

n	σ_a	ξ	10%	5%	1%
10	100	0,2	0,16	0,10	0,03
		0,5	0,15	0,09	0,02
		0,9	0,10	0,05	0,01
	150	0,2	0,31	0,23	0,10
		0,5	0,25	0,16	0,05
		0,9	0,10	0,05	0,01
	200	0,2	0,46	0,37	0,21
		0,5	0,34	0,23	0,09
		0,9	0,10	0,05	0,01
40	100	0,2	0,28	0,19	0,08
		0,5	0,27	0,18	0,06
		0,9	0,11	0,06	0,01
	150	0,2	0,69	0,60	0,42
		0,5	0,62	0,50	0,28
		0,9	0,13	0,07	0,02
	200	0,2	0,89	0,85	0,74
		0,5	0,85	0,76	0,54
		0,9	0,14	0,08	0,02

(4.23)

The power does indeed decrease in line with the kurtosis, i.e. as ξ increases.

4.10. Conclusions

The A_n^2-statistic seems a reasonable enough choice for a control chart procedure to monitor normality in an on-line fashion. It can be implemented in a number of ways, such as

- **Single batch testing**. If samples are available in batches only, A_n^2 can be calculated for each batch, either accepting or rejecting the normality hypothesis for the batch.

- **"Moving" normality testing.** If readings are taken from the production line according to some sampling plan, A_n^2 can be calculated for the last x readings on a continuous basis, meaning that deviation from normality could be picked up sooner.

A_n^2 will be used in Chapter 6 to test normality on a set of data obtained from a manufacturer of detonators.

5. Lot-acceptance Techniques to Control Variance

5.1. Introduction

In Chapter 3 I explained why the variance σ_D^2 of main delay times should be controlled in order to control the probability of reversal. While there exists many simplistic procedures to control the mean of a random variable, existing procedures to control the variance are comparatively complex to implement on a factory floor level, especially when charting is to be done manually by staff members. In this chapter I shall give a general overview of *lot acceptance techniques*, a popular and well-documented method of controlling a characteristic of a distribution. This will be followed by a suggested method of transforming our problem of controlling variance into the much simpler one of controlling a mean with known variance, and I shall make use of said lot acceptance techniques to do just that.

5.2. Overview of lot acceptance

There are two main objectives of acceptance control (see, for example, Hansen (1963) or Bowker (1959)):

- to assure the quality of a particular unit or group of units submitted for acceptance, and

- to assure that the quality over the long term will be consistent with the quality specified.

A lot acceptance procedure can broadly be defined as a procedure for either accepting or rejecting a batch of objects based on the observed characteristics of a certain sample taken from that batch. Two main lot acceptance procedures can be defined, namely:

- inspection by attributes, and
- inspection by variables.

When inspecting a lot based on attributes, one takes a sample from the batch and classify each item in the sample as either *conforming ("working")* or *non-conforming ("not working")*, rejecting the batch when the ratio of non-conforming items in the sample exceeds a pre-determined level.

Many products, however, will have a range of the quality characteristic that will be acceptable, say if the observed characteristic is greater than L but less than U (the one-sided range is a special case of this). The characteristic is thus a random variable with a certain distribution (usually assumed to be Normal(μ, σ^2)) and sentencing of the batch is based on the observed sufficient statistics for the particular distribution ($\bar{x}$ and s^2 in the Normal case).

In the context of batch acceptance procedures, the usual Type I and Type II errors used in hypothesis testing are rephrased as follows:

- *Producers' risk*: The producer is the entity submitting the batch for acceptance testing. Producers' risk therefore represents the risk of a good-quality batch being rejected by the quality control procedure. This is analogous to a Type I error probability, the probability of incorrectly rejecting a correct hypothesis.

- *Consumers' risk*: Similarly, the consumer is the entity that will use the product if the batch is accepted. Consumers' risk therefore represents the risk of not rejecting (i.e. accepting) a batch that does not conform to the set standards. This is analogous to a Type II error in hypothesis testing.

The one major advantage of inspection by variables over inspection by attributes is that the information contained in the sample is used much more efficiently, meaning that smaller samples can be used. Some disadvantages, however, can also be identified, namely:

- heavy dependence on normality of the characteristic in question;

- more advanced technical requirements for the inspection staff;

- the possibility of rejection even though not a single item in the batch sample might be defective.

When developing an inspection plan based on variables, four distinct cases must be examined separately, namely (in increasing order of complexity):

- single specified limit with σ known;
- single specified limit with σ unknown;
- double specified limit with σ known;
- double specified limit with σ unknown;

5.3. Classification of sampling plans

In general, sampling plans can be classified as belonging to one of three main groups, each viewing the objectives of quality control from a slightly different angle:

- *Acceptable Quality Level (AQL)*: The AQL is usually interpreted to refer to the highest percentage defective that is still acceptable as a process average. This means that the AQL is set *a priori* by the producer. Normally, it is defined in such a way that a lot which is at the AQL level has a high probability of acceptance, say $(1 - \alpha)$ for α (the "producer's risk" introduced above) sufficiently small — a typical value for α might be 0.05. The parameter α is usually set at a low level so that the producer has good protection against rejection of submitted lots that are at the AQL level or better. Note that this type of sampling plan classification makes no mention of the protection that the consumer has against the acceptance of a lot **worse** than the AQL.

- *Lot Tolerance Percent Defective (LTPD)*: Where the AQL controls the producer's risk, the LTDP is the friend of the consumer. The LTPD is set by the consumer such that lots submitted from a process that is at the LTPD level (or worse) has a small probability of being accepted (usually defined at or around 0.10). This classification makes no mention of the producer's risk.

- *Point of control*: Where the AQL and LTPD both favour either the producer or the consumer, the point of control seeks to split the risk equally between the two parties, in other words, set the probability of acceptance of a lot that is **at** the point of control equal to 0.5. A submitted lot from a process with a quality **better** than the point of control has a probability **higher** than 0.5 of being accepted, while a lot from a process with a quality **lower** than the point of control has a probability **lower** than 0.5 of being accepted.

5.4. Controlling the variance

Given a random sample $X_1, X_2, \ldots, X_n$ from a $N(\mu, \sigma^2)$ distribution. Define, as usual,

$$\begin{aligned} \bar{X} &:= \tfrac{1}{n} \textstyle\sum X_i \\ S^2 &:= \tfrac{1}{n-1} \textstyle\sum (\bar{X} - X_i)^2. \end{aligned} \tag{5.1}$$

The following results are well-known (for example, see Cassella and Berger

(1990), p.220 for a proof).

- $\bar{X}$ and S^2 are independent random variables.
- $E(S^2) = \sigma^2$ and $var(S^2) = \frac{2\sigma^4}{n-1}$.
- $\bar{X}$ is distributed $N(\mu, \frac{\sigma^2}{n})$.
- The random variable $(n-1)S^2/\sigma^2$ is distributed $\chi^2(n-1)$.

Consider the convergence theorem stated in (2.88). We note that $S^2 \xrightarrow{\mathcal{L}} N(\sigma^2, \frac{2\sigma^4}{n-1})$ and define

$$\begin{aligned} T_n &= S^2 \\ g(\sigma^2) &= \log(\sigma^2) \\ \sigma^2(\sigma^2) &= \tfrac{2\sigma^4}{n-1} \end{aligned} \tag{5.2}$$

so that, by (2.88),

$$\begin{aligned} \log S^2 &\approx_{\mathcal{L}} N(\log \sigma^2, \tfrac{2}{n-1}) \\ &=_{\mathcal{L}} \tfrac{1}{n-1} \textstyle\sum_{i=1}^{n-1} U_i \text{ where } U_i =_{\mathcal{L}} N(\log \sigma^2, 2). \end{aligned} \tag{5.3}$$

This indicates that $\log S^2$ is approximately equal in distribution to the average of $n-1$ samples from a normal distribution with mean $\log \sigma^2$ and constant variance 2. As we have noted in the introduction to this chapter, batch acceptance techniques that inspect the mean are well-developed, raising the possibility of using such techniques to inspect the sample variance.

Since the true underlying variance σ^2 is unknown, we can start by setting an *a priori* upper limit σ_0^2 which we define to be the maximum allowable variance. We now have to develop some kind of decision rule of the form

$$\text{accept lot if } \log(S^2) < \kappa \tag{5.4}$$

for some suitable κ.

Furthermore, we want

$$P(\log(S^2) < \kappa \mid \sigma^2 = \sigma_0^2 + \Delta), \tag{5.5}$$

the probability of (incorrectly) accepting the batch given the variance is larger than our specified upper limit, to be small, say

$$P(\log(S^2) < \kappa \mid \sigma^2 = \sigma_0^2 + \Delta) = \alpha \tag{5.6}$$

for some small α and Δ.

However, we don't want to unnecessarily reject a "good" batch either, so that we require

$$P(\log(S^2) < \kappa \mid \sigma^2 = \sigma_0^2) = 1 - \beta \tag{5.7}$$

for some small β.

Note that from (5.3),

$$\begin{aligned} & P(\log(S^2) < \kappa \mid \sigma^2) \\ = \; & \Phi\left(\frac{\kappa - \log\sigma^2}{\sqrt{\frac{2}{n-1}}}\right). \end{aligned} \tag{5.8}$$

Given the above set of limitations, we are in a position to solve for the unknown κ, as well as the other (implicitly) unknown parameter n, the size of the sample that we have to take from the batch to calculate $\log(S^2)$. Formally, given

$$\sigma_0^2 < \sigma_0^2 + \Delta := \sigma_1^2 \text{ and "small" } \alpha \text{ and } \beta$$

we want to find κ and n such that

$$\Phi\left(\frac{\kappa - \log\sigma_1^2}{\sqrt{\frac{2}{n-1}}}\right) = \alpha \quad \text{and} \quad \Phi\left(\frac{\kappa - \log\sigma_0^2}{\sqrt{\frac{2}{n-1}}}\right) = 1 - \beta. \tag{5.9}$$

Dividing the two equations in (5.9) yields

$$\begin{aligned} \frac{\kappa - \log\sigma_0^2}{\kappa - \log\sigma_1^2} &= \frac{\Phi^{-1}(1-\beta)}{\Phi^{-1}(\alpha)} \\ \Rightarrow \qquad \kappa &= \frac{\Phi^{-1}(1-\beta)\log\sigma_1^2 - \Phi^{-1}(\alpha)\log\sigma_0^2}{\Phi^{-1}(1-\beta) - \Phi^{-1}(\alpha)}. \end{aligned} \tag{5.10}$$

Similarly,

$$\begin{aligned} \log\sigma_0^2 + \sqrt{\tfrac{2}{n-1}}\Phi^{-1}(1-\beta) &= \log\sigma_1^2 + \sqrt{\tfrac{2}{n-1}}\Phi^{-1}(\alpha) \\ \Rightarrow \qquad n &= 2\left(\tfrac{\Phi^{-1}(1-\beta)-\Phi^{-1}(\alpha)}{\log\sigma_1^2/\sigma_0^2}\right)^2 + 1. \end{aligned} \tag{5.11}$$

Example 3. *Consider the following case.*

$$\begin{aligned} \sigma_0 &= 40 \\ \sigma_1 &= 50. \end{aligned} \tag{5.12}$$

The following tables show n and κ for various possibilities of α and β.

n / α	β 15,0%	12,5%	10,0%	5,0%	2,50%
10,0%	28	31	34	44	54
7,5%	32	35	38	49	59
5,0%	37	40	44	55	66
2,5%	46	50	54	66	78
1,0%	58	62	66	80	93
0,5%	67	71	76	90	104

(5.13)

κ / α	β 15,0%	12,5%	10,0%	5,0%	2,50%
10,0%	7,58	7,59	7,60	7,63	7,65
7,5%	7,56	7,58	7,59	7,62	7,64
5,0%	7,55	7,56	7,57	7,60	7,62
2,5%	7,53	7,54	7,55	7,58	7,60
1,0%	7,52	7,53	7,54	7,56	7,58
0,5%	7,51	7,52	7,53	7,55	7,57

(5.14)

As an example of using the tables, we note that for $\beta = 15\%$ and $\alpha = 5\%$, we shall need to sample 37 values, calculate $\log S^2$ and compare this with the critical

value $7,55$. *If the calculated value of* $\log S^2$ *is less than this critical point, we conclude that the variance of the batch is in control on the* 5% *level of significance.*

Chapter 6 contains further examples of how this method can be applied in controlling the variance of detonator delay times.

6. Data analysis

I obtained 20 samples of size 50 from a manufacturer of main delays. The delays are manufactured according to the specification $\mu_D = 4\ 500ms$. The standard deviation σ_D was not specified. Figures (6.1) and (6.2) depict the means and standard deviations of the 20 samples.

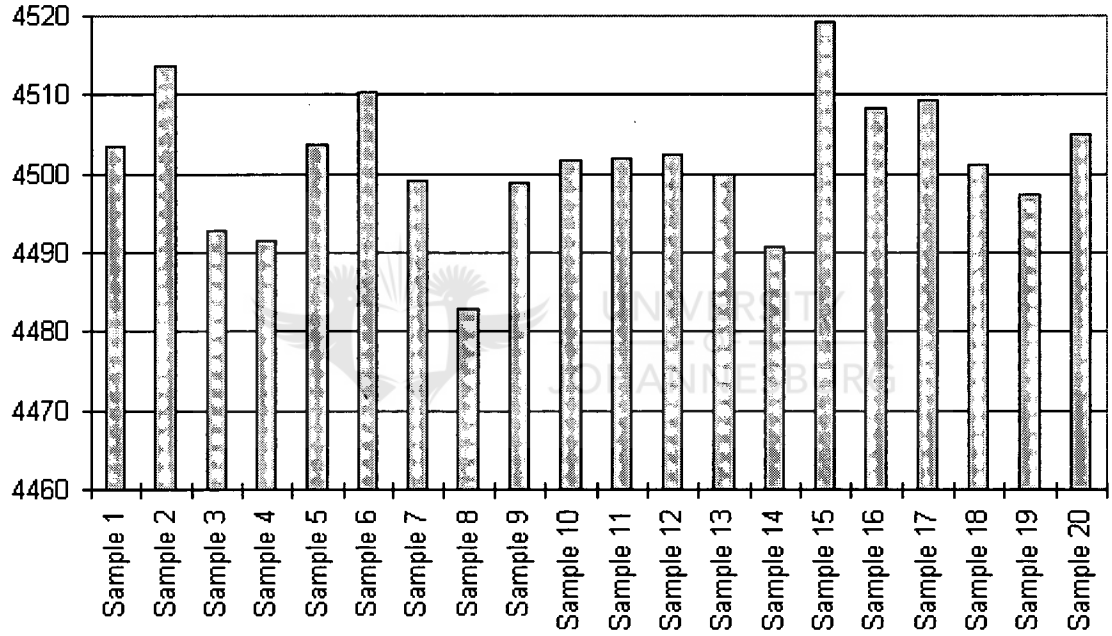

Figure 6.1: Means of samples.

6.1. Testing normality

As a first step we should analyse the validity of assuming the delay times are normally distributed. Figure (6.3) depicts the observed A_n^2-statistics for the 20

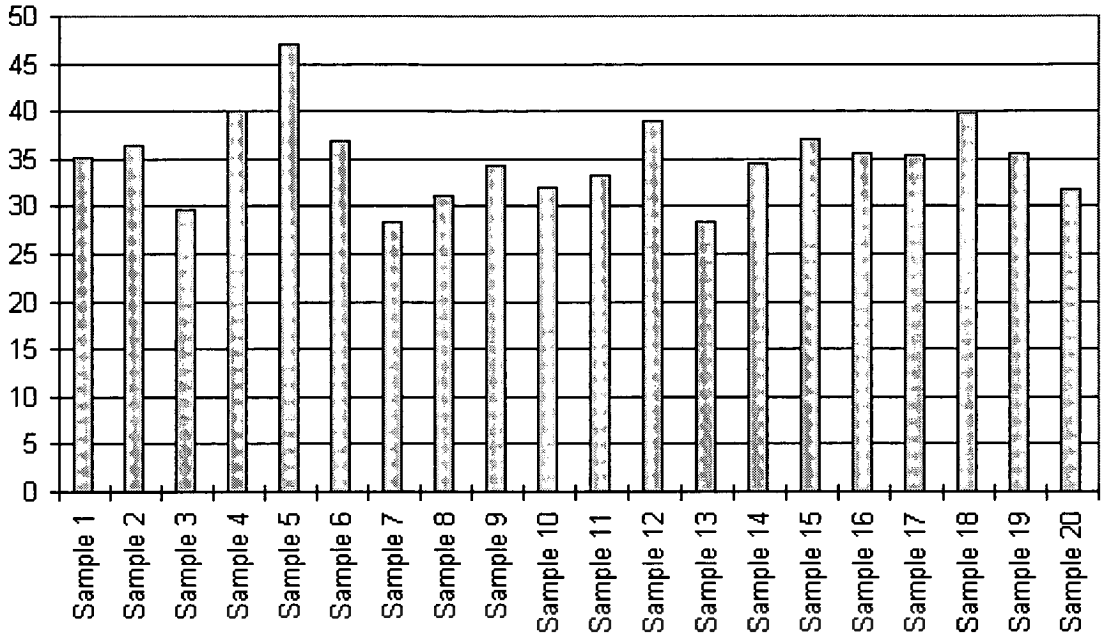

Figure 6.2: Standard deviations of samples.

samples against certain critical points.

There doesn't seem to be too much evidence that would suggest non-normality, except possibly for samples 8 and 17. Figures (6.4) and (6.5) depict normal quantile plots for the two samples in question.

From the quantile plots there would seem to be some systematic deviation from normality in the tail areas, and for this reason I shall exclude these two samples from the calculations to follow.

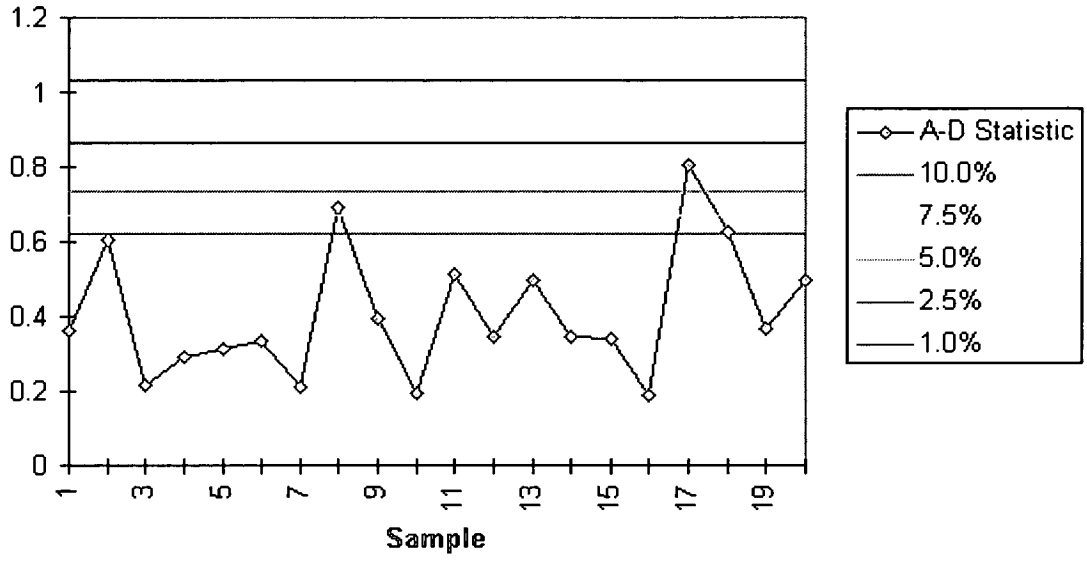

Figure 6.3: Observed A_n^2-statistics against critical points.

6.2. Estimating the detonation process parameters

Pooling the remaining 18 samples together to obtain readings $D_1, D_2, \ldots, D_{900}$, we can calculate the following unbiased point estimators:

$$\begin{aligned} \hat{\mu}_D &= \tfrac{1}{900} \sum D_i &&= 4\,502,3 \\ \hat{\sigma}_D &= \sqrt{\tfrac{1}{899} \sum (D_i - \hat{\mu}_D)^2} &&= 35,95. \end{aligned} \tag{6.1}$$

Using (2.60) we can estimate the pairwise probability of reversal when these main delays are used with surface delays with mean μ_d and standard deviation σ_d. The following table gives $\widehat{P_{rev}}$ for various combinations of surface delay para-

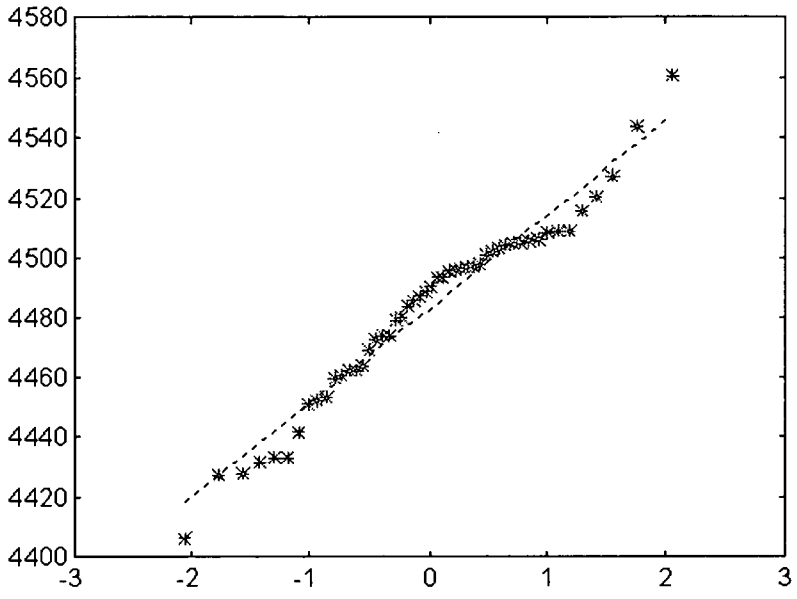

Figure 6.4: Normal quantile plot for sample 8.

meters:

	$\sigma_d = 2$	$\sigma_d = 4$	$\sigma_d = 6$
$\mu_d = 200$	$4,23 \times 10^{-5}$	$4,40 \times 10^{-5}$	$4,70 \times 10^{-5}$
$\mu_d = 300$	$1,86 \times 10^{-9}$	$2,02 \times 10^{-9}$	$2,31 \times 10^{-9}$

(6.2)

Using (2.61) we can estimate $P(R)$, the probability of a reversal somewhere in a sequence of detonators for various sequence lengths n, with n being the number

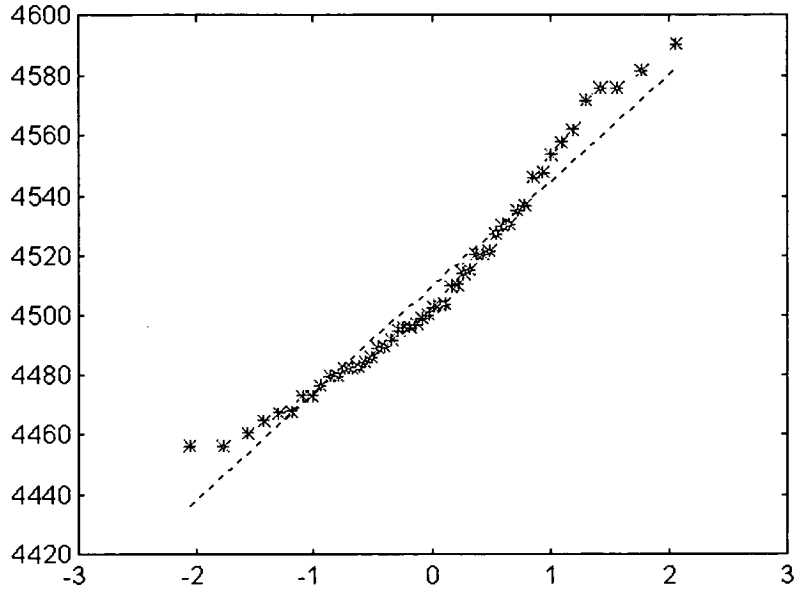

Figure 6.5: Normal quantile plot for sample 17.

of surface delays in the sequence (or alternatively, the number of main delay pairs).

$n = 100$	$\sigma_d = 2$	$\sigma_d = 4$	$\sigma_d = 6$
$\mu_d = 200$	$4,22 \times 10^{-3}$	$4,39 \times 10^{-3}$	4.67×10^{-3}
$\mu_d = 300$	$1,86 \times 10^{-7}$	$2,02 \times 10^{-7}$	$2,31 \times 10^{-7}$
$n = 200$	$\sigma_d = 2$	$\sigma_d = 4$	$\sigma_d = 6$
$\mu_d = 200$	$8,43 \times 10^{-3}$	$8,76 \times 10^{-3}$	$9,31 \times 10^{-3}$
$\mu_d = 300$	$3,72 \times 10^{-7}$	$4,04 \times 10^{-7}$	$4,63 \times 10^{-7}$

(6.3)

We can reduce the bias in $\widehat{P_{rev}}$ by using the Jackknife procedure as described

in (2.75). This yields the following estimators:

	$\sigma_d = 2$	$\sigma_d = 4$	$\sigma_d = 6$
$\mu_d = 200$	$4,02 \times 10^{-5}$	$4,18 \times 10^{-5}$	$4,45 \times 10^{-5}$
$\mu_d = 300$	$1,34 \times 10^{-9}$	$1,47 \times 10^{-9}$	$1,70 \times 10^{-9}$

(6.4)

Comparing (6.4) with (6.2), it is clear that $\widehat{P_{rev}}$ overestimates the true P_{rev}, with the degree of overestimation increasing as μ_d increases.

7. Notation, abbreviations and constants

$=_{\mathcal{L}}$	Equal in distribution.
$A = \{event\}$	An event A.
$P(A)$	Probability of the event A.
$N(\mu, \sigma^2)$	Normally distributed with parameters μ and σ^2.
$U[0;1]$	The uniform distribution.
Z	Standard normal distribution, i.e. $Z =_{\mathcal{L}} N(0,1)$.
$\Phi(x)$	$P(Z \leq x)$.
$\phi(x)$	$\Phi'(x)$.
Z_α	α-percentage point of Z, i.e. $\Phi^{-1}(1-\alpha)$
R_i	The event $\{A$ *reversal occurs at* ith *detonator pair*$\}$.
$P(R_i) = P_{rev}$	Pairwise probability of reversal.
$P(R)$	Probability of reversal somewhere in blasting sequence.
$\lambda = \frac{-\mu_d}{\sqrt{\sigma_d^2 + 2\sigma_D^2}}$	The argument used throughout in P_{rev}
$\lfloor x \rfloor$	The integer part of x, e.g. $\lfloor 3.1415 \rfloor = 3$.
$\lceil x \rceil$	The least integer not smaller than x, e.g. $\lceil 3.1415 \rceil = 4$.
$\aleph$	The set of natural numbers, i.e. $\{1, 2, 3, \ldots\}$.
A'	The transpose of matrix A.

8. References

1. Anderson, T.W. and Darling, D.A. (1952). Asymptotic Theory of Certain 'Goodness of Fit' Criteria Based on Stochastic Processes. *Annals of Mathematical Statistics*, **23**, 193-212.

2. Anderson, T.W. and Darling, D.A. (1954). A Test of Goodness of Fit. *Journal of the American Statistical Association*, **47**, 765-769.

3. Bowker, A.H. and Lieberman, G.J. (1959). *Engineering Statistics*, Englewood Cliffs: Prentice-Hall Inc.

4. Cassella, G. and Berger, R.L. (1990). *Statistical Inference.* Belmont: Wadsworth & Brooks/Cole.

5. Chernoff, H. and Lehmann, E.L. (1954). The Use of Maximum Likelihood Estimates in χ^2 Tests for Goodness of Fit. *Annals of Mathematical Statistics*, **25**, 579-586.

6. Feller, W (1968). *An Introduction to Probability Theory and its Applications, Volume I.* New York: John Wiley & Sons.

7. Grimmett, G.R. and Stirzaker, D.R. (1992). *Probability and Random Processes.* Oxford: Clarendon Press.

8. Hansen, B.L. (1963). *Quality Control: Theory and Applications.* Englewood Cliffs: Prentice-Hall Inc.

9. Kac, M., Kiefer, J. and Wolfowitz, J. (1955). On Tests of Normality and Other Tests of Goodness of Fit Based on Distance Methods. *Annals of Mathematical Statistics*, **26**, 189-211.

10. Lilliefors, H.W. (1967). On the Kolmogorov-Smirnov Test for Normality with Mean and Variance Unknown. *Journal of the American Statistical Association*, **62**, 399-402.

11. Mann, H.B. and Wald, A. (1942). On the Choice of the Number of Class Intervals in the Application of the Chi Square Test. *Annals of Mathematical Statistics*, **13**, 306-317.

12. Massey, F.J. (1951). The Kolmogorov-Smirnov Test for Goodness of Fit. *Journal of the American Statistical Association*, **46**, 68-78.

13. Miller, R.G. (1974). The Jackknife — A Review. *Biometrika,* **61**, 1-15.

14. Petrov, A.A. (1956). Verification of Statistical Hypotheses on the Type of Distribution Based on Small Samples. *Theory of Probability Applications*, **1**, 223-245.

15. Prohorov, Y. (1966). Some Characterization Problems in Statistics. *Proceedings of the Fifth Berkeley Symposium on Mathematical Statistics and Probability*, **1**, 341-349.

16. Quenouille, M.H. (1956). Notes on Bias in Estimation. *Biometrika,* **43**, 353-360.

17. Quesenberry, C.P., Whitaker, T.B. and Dickens, J.W. (1976). On Testing Normality Using Several Samples: An Analysis of Peanut Aflatoxin Data. *Biometrics*, **32**, 753-759.

18. Rao, C.R. (1965). *Linear Statistical Inference and Its Applications.* New York: John Wiley & Sons.

19. Ruppert, D. (1987). What Is Kurtosis? *American Statistician*, **41**, 1-5.

20. Shorack, G.R. and Wellner, J.A. (1986). *Empirical Processes with Applications to Statistics.* New York: John Wiley & Sons.

21. Stephens, M.A. (1976). Asymptotic Results for Goodness of Fit Statistics with Unknown Parameters. *American Statistician*, 4, 357-369.

22. Trollip, L.E., Espley-Jones, R.C., Ehmke, C.W., Lessing, I.J. and Bozalek, S.J. (1967). Igniter Cord and Safety Fuse in Sequential Firing. *Journal of the SA Institute of Mining and Metallurgy*, **July 1967**, 679-682.